This is to certify that the

thesis entitled

A METHOD FOR ANALYZING THREE-DIMENSIONAL HUMAN WRIST MOTION USING A JOINT COORDINATE SYSTEM

presented by

John Timothy Zipple

has been accepted towards fulfillment
of the requirements for

MASTER'S degree in BIOMECHANICS

Major professor

Date 11-8-89

A METHOD FOR ANALYZING THREE-DIMENSIONAL HUMAN WRIST MOTION USING A JOINT COORDINATE SYSTEM

By

John Timothy Zipple

A THESIS

Submitted to
Michigan State University
in partial fulfillment of the requirements
for the degree of

MASTER OF SCIENCE

Department of Biomechanics
College of Osteopathic Medicine

1989

ABSTRACT

The purpose of this study was to provide a methodology for the analysis of three dimensional motion of the human wrist using a three degrees-of-freedom model. A multiple camera video system was synchronized with a dynamic image video processor. Filmed at 60 hertz, the data were digitized automatically by a computer software program which calculated target centroids from pixel-perfect video images. The technique for analyzing motion involved a non-invasive, surface-targeting scheme on the wrist and forearm, using retro-reflective tape. Local segment coordinate systems were formed and wrist motion about a non-orthogonal coordinate system was calculated using Euler angles. Knowledge of wrist kinematics will be an important tool in the studies of human upper extremity function in activities of daily living (ADL's). This study was supported in part by the National Foundation for Food and Pharmacological Packaging Research to model wrist action when opening child-resistant medicine caps.

DEDICATION

I wish to dedicate this work to the three most important women in my life; to my wife Nancy, who tolerated my crazy schedules and obsessive-compulsive behavior, to my daughter Monica, who was born during the writing of this thesis and provided disruptions in my circadian rhythms and a reason to work hard to finish, and to my mother Joan K. Zipple who died in September of 1989, she gave me love and encouragement for 28 years and I miss her deeply.

ACKNOWLEDGEMENT

I wish to thank the following individuals for their generous support and sharing of knowledge that made this work possible. First, to my teachers and advisors: Robert Soutas-Little PhD., Roger Haut PhD., Herbert (Mac) Reynolds PhD., Robert Hubbard PhD., James Rechtien D.O., PhD, and Dianne Ulibarri PhD., thanks for giving me a piece of your minds. Secondly, to the secretaries: Sharon Husch, LeAnn Slicer, and Brenda Robinson, thanks for keeping me on schedule and for "showing me the ropes". Finally, thanks to Cliff Beckett, my technical advisor , and to the biomechanics students too numerous to mention, I learned as much from your wealth of ideas as I did from my courses.

TABLE OF CONTENTS

LIST OF TABLES

TABLE OF FIGURES

INTRODUCTION

The wrist, or carpus, is a deformable anatomic entity composed of eight small carpal bones (scaphoid, lunate, triquetrum, pisiform, hamate, capitate, trapezium, and trapezoid) and the surrounding supportive structures. These soft tissue structures include the tendons that cross and/or attach within the carpus, and those ligamentous structures that connect the carpal bones to each other and to the bony elements of the hand and forearm.

The wrist functions both kinetically by transmitting forces from the hand to the forearm and from the forearm to the hand, and kinematically by allowing changes in the location and orientation of the hand relative to the forearm (Taleisnik, 1985). In order to understand this complex joint, the wrist was modeled as an unknown mechanism connected between two rigid bodies: the hand and the forearm. In the joint kinematic analysis of three-dimensional motion between rigid bodies, it is necessary to obtain the position history of a minimum of three non-colinear points. Therefore, a reliable experimental apparatus is required to continuously monitor the positions of these non-colinear points in the rigid bodies. By setting up local coordinate systems on the hand and forearm

and by using Euler angles (Goldstein, 1960) to analyze the motions between the two rigid body segments, this study provided a reliable way of capturing human wrist kinematics.

The relative position and attitude of body segments connected by an anatomical joint may be measured by a variety of methods. Various investigators have used stereoscopic and plain roentgenograms (Brumbaugh, Crowninshield, Blair, & Andrews, 1982; Bryce, 1896), plaster molds and dissections, still and high speed cine photography (Carr, 1989; Chao & Morrey, 1978; Grood & Suntay, 1983; Soutas-Little, Beavis, Verstraete, & Markus, 1987), and sonic digitizers, using a range of two to six degrees-of-freedom modeling systems. Since the complex motions of the human wrist occur in three-dimensions, the data in this study were collected on the Sun-4 Motion Analysis System, using a three-camera, video-synchronized set-up. This system has an automated digitization software program, which decreased the incidence of human error and sped up data analysis.

REVIEW OF LITERATURE

A complete understanding of wrist joint kinetics and kinematics is necessary for: an objective analysis of human wrist function during activities of daily living (ADL's), for comparison of endoprosthetic joint replacements, and for diagnosis of traumatic or pathologic joint disorders.

In defining two-dimensional range of motion of the wrist, various authors (DeBrunner, 1982; Heck, Hendryson, & Rowe, 1965; Hoppenfeld, 1976; Polley & Hunter, 1978) have reported different values. These normal (average) ranges of motion were based on clinical measurements of wrist motion using a standard goniometer (a protractor with two extended arms). Although triaxial electrogoniometers provide three dimensional rotation measurements, the accuracy of these techniques needed to be verified (Chao & Morrey, 1978). There was a possibility of human error introduced in these two techniques of motion measurement, depending on placement and/or fixation of the goniometer to the body (Chao, 1980).

The movements included in circumduction of the wrist, which were analyzed for this work, were defined by Kapandji (1985) as the combination of the movements of flexion, extension, adduction, and abduction. The motions take place simultaneously about the two axes of the wrist in anatomical

position. The transverse axis (AA') and the antero-posterior axis (BB') of the wrist are shown in Figure 1 and the definitions of the individual motions of the wrist are as follows;

1. Flexion (arrow 1): the ventral (palmar) surface of the hand moves towards the ventral aspect of the forearm.
2. Extension (arrow 2): the dorsal (back) surface of the hand moves towards the dorsal aspect of the forearm.
3. Ulnar deviation or adduction (arrow 3): the hand moves towards the axis of the body and its medial (ulnar) border forms an obtuse angle with the ulnar bone of the forearm.
4. Radial deviation or abduction (arrow 4): the hand moves away from the axis of the body and its lateral (radial) border forms and obtuse angle with the radial bone of the forearm.
5. Circumduction: the hand moves in a conical path with apex at the wrist as all four of the previous motions are combined.

Early functional analysis of carpal bone complex modeling resulted in several conceptual types. In a model by Fick (1910), the proximal and distal row of carpal bones, each as a fixed group were thought to rotate around a fixed axis in both flexion and deviation of the hand. In a study by Gilford, Bolton, and Lambrinudi (1943), they proposed

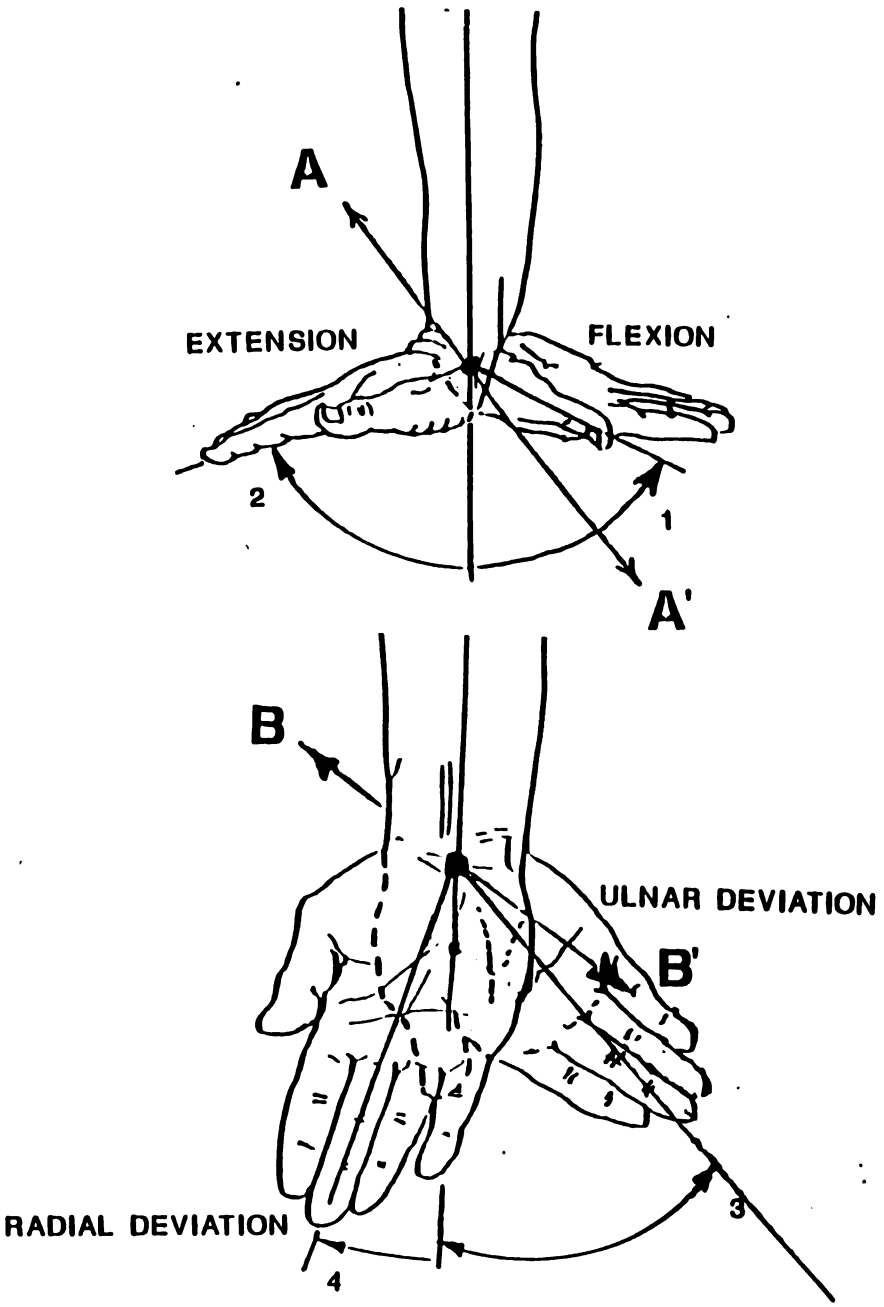

Figure 1: Motions About the Two Wrist Axes

that the wrist joint performed as a system of three longitudinal chains of which the capitate-lunate-radius chain formed the central part. Contrary to the fixed row concept, the longitudinal chain concept stimulated synchronous movement of the carpal bones during flexion, explained through the actions of the scaphoid, which bridges the proximal and distal bones in the central chain (Gilford et al., 1943).

In a study by DeLange, VanLeeuwen, Kauer, and Huiskes (1984), the authors attempted to obtain kinematic information about the individual carpal bones during flexion of the hand of one human specimen. Using a roentgen stereophotogrammetric system, DeLange et al. proposed to clear up the discrepancies between the fixed row and the longitudinal chain models.

DeLange et al. (1984) stated that the distal carpal row performed nearly the same flexion excursions during flexion and extension and therefore can be approximated as a fixed row concept. The proximal carpal bones however showed different flexion angles which was contrary to the fixed row concept. Secondly, they found that both carpal rows moved synchronously and uniformly, supporting the longitudinal chain concept of Fick (1910).

The contributions of the intercarpal and radiocarpal joints to the total arc of flexion differ in the three longitudinal chains: radius-scaphoid-trapezoid (R-S-T), radius-lunate-capitate (R-L-C), and ulna-triquetrum-hamate

(U-T-H) (DeLange et al., 1984). It was concluded by DeLange et al. that for the medial (U-T-H) as well as for the lateral (R-S-T) chain, the radiocarpal joint contributed most to the total arc of flexion. In the central chain, this was also true for the intercarpal joint. Hence, treatments of the proximal and distal carpal rows as fixed units appeared incorrect.

Investigations by Volz, Lieb and Benjamin (1980) and Youm and Flatt (1980) found different results from DeLange et al. (1984) when comparing carpal movement. While both studies found that both the radiocarpal and intercarpal joints contributed to all phases of flexion-extension motion of the wrist, the contributions of the proximal and distal carpal rows to radial and ulnar deviations were found to be different. Volz et al. (1980) stated that with radial and ulnar deviation, the proximal and distal rows moved in opposite directions with the distal row being displaced toward the direction of the hand deviation.

Youm and McMurty (1978) found no proximal carpal row movement with radial deviation, while ulnar deviation resulted in motion of both the intercarpal and the radiocarpal joints.

In another anatomical joint model proposed by Sommer and Miller (1980), the authors used the optimization technique to estimate the separation of, and the angle between the two axes of a universal joint with skew-oblique revolutes as a biomechanical wrist model.

In wrist analysis, there was confusion surrounding the location of the center of rotation for radial and ulnar deviation of the hand relative to the forearm in subjects with non-pathologic wrists. Kapandji (1985) stated that this center of rotation lies between the lunate and the capitate, where Volz et al. (1980) contended that it remained in the head of the capitate. Wright (1935) stated that the center is in the head of the capitate for radial deviation and in the waist or neck of the capitate during ulnar deviation.

The center of rotation for flexion and extension motion of the wrist is also controversial. Kapandji (1985) believed that there were two parallel and closely spaced axes of rotation located in the radiocarpal and midcarpal joints. Volz et al. (1980) and MacConaill (1941) each stated that there was a single axis of rotation that remained in the head of the capitate. Wright (1935) also believed that the center of the rotation was located in the head of the capitate during flexion, but stated that for extension, the center lies at the intercarpal joint.

With the advancements in the field of knowledge of the biomechanics of the wrist, several authors have attempted to use certain hand-wrist parameters to diagnose internal disease or derangement. Youm and Flatt (1980) believed that the carpal height (the distance from the base of the third metacarpal to distal articular surface of the radius) was

constant throughout radial-ulnar deviation of the normal wrist and could be used as a measure of carpal collapse.

Wrist joint replacement, limited and total wrist arthrodesis, and proximal row carpectomy are common operative procedures for disorders involving the wrist. In an effort to evaluate the effects of these common operative procedures, several in-vivo and in-vitro investigations have been performed by Mann, Werner, and Palmer (1989) to examine the motion of the wrist during various functional activities. Using a frequency spectral analyzer, they found that the average predominant frequency component of these activities of daily living (ADL's) was approximately 1 Hz, with 75% of the spectral energy less than 5 Hz. The authors felt that spectral analysis would be of value in the development of a wrist motion simulator, which required sufficient frequency response to track desired wrist motion.

In the developing field of biomedical engineering, prosthetic wrist replacements are becoming more common as a means to decrease pain, maintain range of motion, and restore functional ability. The purpose of a study by Tolbert, Blair, Andrews, and Crowninshield (1985) was to describe normal wrist kinetics and investigate the in-vitro kinetics of four currently available wrist prostheses named the Swanson, the Meuli, the Volz, and the Hamas. The authors found that the total wrist prostheses examined were unable to reproduce normal wrist kinetics. Perhaps human wrist motion is impossible to imitate by mechanical means.

The purpose of this research was to provide a method for accurately analyzing human wrist rotations in three dimensions using a joint coordinate system. This method has been used in previous studies (Grood & Suntay, 1983; Chao & Morrey, 1978; Soutas-Little, et al., 1987; Carr, 1989) for analysis of the three-dimensional joint motions of the knee, elbow, ankle, and temporo-mandibular joints respectively. DeLange, VanLeeuwen, Kauer, Huiskes and Huson (1983) used stereoradiography to record the movements of each of the carpal bones. Three non-colinear tantalum pellets in each bone were used to set up local coordinate systems to calculate the rotations (Euler angles) and translations of the carpal complex in three dimensions.

METHODOLOGY

The methodology developed and utilized in this study provided a routine for the analysis of wrist motion. The methodology was designed around the use of the Sun-4 Motion Analysis System which was operational in May, 1989.

I) DEVELOPMENT OF THE CALIBRATION STRUCTURE

The pre-existing calibration structures in the laboratory were designed for the calibration of a space for lower body or total body motion analysis. The motion of the relatively smaller hand and forearm body segments occurred in a controlled area of approximately one cubic foot, and therefore, construction of a new calibration structure was necessary. Design and materials specifications for the calibration structure were suggested by Walton (1989). The calibration structure frame was fabricated from half inch plexiglass plates and one inch plexiglass rods. Ultra-flat black paint was used to cover the frame in order to decrease the reflectivity of the surfaces of the plexiglass. The targets used as control points were 0.75 inch brass ball bearings covered with 3M Scotchlite Brand High Gain 7610 Sheeting (retro-reflective tape)(see Figure 2). Retro-reflective tape has a reflectivity 1600 times the

Figure 2: Target Fabrication Materials

reflectivity of a piece of white paper and provided clear pixel-imaging for digitization.

The target spacers were brass tubes, machined and painted with ultra-flat black enamel. To prevent variation in the lengths of the target-hanging system, surveying thread was used. The calibration structure was leveled, utilizing three leveling bolts on the undersurface of the frame and a circle-level on the top plate. The level top plate of the frame provided an accurate X-Y plane for motion analysis. For an illustration of the structure, refer to Figure 3.

Figure 3: The Calibration Structure

Calibration of the structure was accomplished using a vernier caliper and an anthropometer to measure the target diameters, the target spacer lengths and the distances between the holes on the undersurface of the top plate of the frame. Measurements of the calibration space were accurate to within 1.0 millimeter because the anthropometer allowed measurements in millimeter increments. The computer software has an environmental operator which gave values to the targets (environmental variables) during calibration of the space where motion took place. A measure of the accuracy of the values of the three-dimensional coordinates of the targets given to the computer was reported as the parameter: "norm of residuals". The residual value of less than 0.3 calculated for all cameras fell below the system requirements for residual values of less than 2.0 indicating an accurate calibration space.

II) TARGETING SCHEME

The targeting of the human wrist for analysis of motion may be variable, depending on the intricacies of the motion that is being examined. For the purposes of this study, a relatively simple scheme was chosen to target the two "rigid" body segments of the wrist and hand. For an illustration of the targeting scheme, refer to Figure 4. Plastic beads covered with 3M Scotchlite Brand High Gain 7610 Sheeting (retro-reflective tape) and glued to a nuagahyde backing were attached to the hand using double-sided, non-allergetic tape. The targets weighed an average of 0.85 grams each and did not interfere with wrist motion. In an attempt to minimize the soft tissue movement error of the hand and forearm, the majority of the targets were placed over bony prominences.

The spherical retro-reflective targets were attached to the following skin surfaces of the right forearm and hand; 1) mid-forearm, midway between the ulna and radius, 2) dorsal surface of radial styloid, 3) head of the capitate, 4) dorsal surface of ulnar styloid, 5) second metacarpal head, and 6) third metacarpal head. The photographic representation of this targeting scheme is illustrated in Figure 4.

III) DEFINITION OF JOINT COORDINATE SYSTEM

An experimental protocol developed by Grood and Suntay

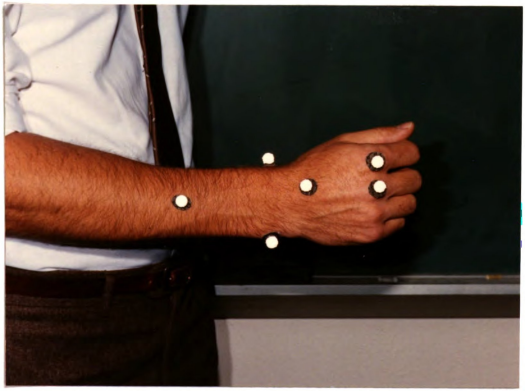

Figure 4: Targeting Scheme

analyze foot motion during gait, used a method of measuring three-dimensional rotation of one rigid body relative to another through use of two coordinate systems. This system of Euler angles used one coordinate system attached to the object and one attached to the laboratory to measure rotations about one axis on each system and the third rotation about a floating axis. The floating axis was calculated by a cross product of the axes from the two coordinate systems.

By modeling the hand and forearm as two rigid bodies and by applying the local segment coordinate system to the three-dimensional target data, relative joint angle motion was determined. Specifically, wrist flexion and extension, and radial deviation and ulnar deviation about the two axes of motion were analyzed. Supination and pronation, which are defined in the analytical methods section, were also analyzed.

IV) EXPERIMENTAL PROTOCOL

An experimental protocol was established to measure three dimensional motion of the hand about the joint coordinate reference axes. Video data collection involved the use of three solid-state, shuttered, video cameras. Data were collected at 60 frames per second at one millisecond per frame. The data from the three cameras were synchronized by an advanced VP-320 model dynamic image processor.

The filming of the motion of the human hand was performed at the Biomechanical Evaluation Laboratory of Michigan State University at Saint Lawrence Hospital in Lansing, Michigan on August 2nd, 1989.

The subject was a 28 year old, white male with no previous associated medical history and no history of traumatic injury to his right upper extremity. The subject reported that he was right handed and the targeting was performed on the right hand and forearm in accordance with the targeting scheme previously defined.

The small plastic beads were chosen as targets because of their size compared to the relatively small surface area of the human hand and to prevent target cross-over with the software tracking program. Cross-over of the reflective targets becomes a problem while tracking the hand with this automated digitizing program because as the targets overlap each other on the two-dimensional video image, the targets merge and the centroid is calculated for the merged spheres as if they were a single target.

Target size was also of major concern since the automated digitizing system of target tracking is quite different from the high speed cine-photogrammetric techniques previously used for motion analysis. The Expertvision three-dimensional (EV3D) software digitizing program sweeps across a grid of pixels on the video image (240 height x 256 width pixels) and averages the centroid of each sweep to find the centroid of the target. Therefore,

larger targets provide a greater pixel surface area from which to average. Traditionally, the high speed cine-photogrammetric techniques have benefited from a smaller target size to minimize human error in digitizing. Since digitization is automatic with the system used, the concern for target size was that they had to be small enough to decrease the incidence of target cross-over and large enough to give an accurate video image for an automated centroid calculation.

The three recording video cameras were brought in close to the subject's targeted extremity to provide the tracking system an adequate pixel number to find a centroid. The three cameras were spaced approximately 91.44 cm. from the center of the calibrated space and at 45 degree angles from the surface of the subject's arm. This set-up was adequate for capturing the movement patterns selected for analysis. The cameras are shown in their respective positions in Figure 5. Note that the height of the three cameras was equal (156.2 cm.).

Illumination for the retro-reflective targets was provided by flood lights attached approximately two inches from the center of the camera lens. The proximity of the flood light to the lens enabled the tape to reflect light at maximum intensity since the reflected light is sensitive to observation angle. The observation angle is the angle between the incidence light ray, the reflective target, and the reflective ray reaching the camera lens. Each increase

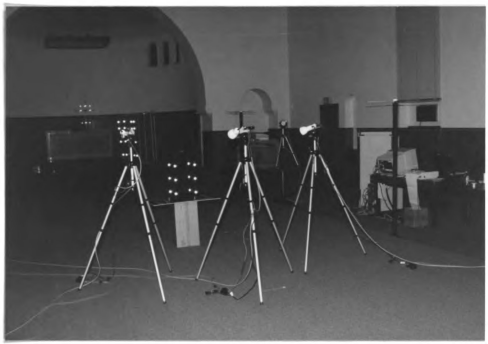

Figure 5: Camera Positioning

of one degree of observation angle, reduces the intensity of the reflected light by a factor of 16 (3M Products Bulletin, 1989). Therefore, the light source needs to be close enough to the lens to create the smallest observation angle, yet far enough away to prevent thermal distortion or damage to the lens and camera.

The sequence for data acquisition began with the filming of the calibration structure. A lab coordinate system with origin at the corner of a horizontal plane connecting the four bottom targets was established and the exact three-dimensional locations of the calibration targets were calculated by the EV3D software program. Video taping of the static structure allowed the EV3D program to calibrate the necessary transformation coefficients for a

direct linear transformation, enabling the three-dimensional positions of the targets to be calculated during the motion sequence (Walton, 1981).

The subject was instructed to stand next to the table on which the calibration structure was previously positioned, with his right hand and forearm in the calibrated space. The right upper extremity was positioned in 90 degrees of elbow flexion with the forearm in a neutral position (midway between supination and pronation with thumb facing superiorly). Data were collected for five seconds at 60 hertz as the subject performed circumduction of the targeted wrist. The sequence of individual motions of the wrist was: extension, ulnar deviation, flexion, and radial deviation. This sequence was performed for two trials at the subject's natural rhythm of approximately one to two hertz. Two trials each of simple flexion-extension and radial-ulnar deviation motions were collected with the subject attempting to follow a single plane of motion for each trial.

The three-dimensional position data for each target were computed by the software program developed by Walton (1981). The necessary direct linear transformations were performed using the calibration coefficients determined in the environment operator program. The environment program functions to set the internal system environment by giving values to the environment variables, thus providing a calibrated space in which the wrist motion can be analyzed. The three-dimensional coordinates recorded in centimeters

are shown in Table 1. Frame number and time in milliseconds were included with the position data.

V) ANALYTICAL METHODS

Analysis of the three-dimensional position data involved the use of several EV3D software subprograms and a joint coordinate system program to adequately represent the wrist motion of the subject. For an animated stick-figure modeling of the wrist, the position data were tracked using the three-dimensional tracking program.

The tracking program functions to track objects moving in three-dimensional object space by computing 3-D paths from two or more time-matched video files (Motion Analysis Corporation, 1987). By intializing the data points, a set of targets were identified in a single frame of data to check the correspondence among the cameras' images. This automated digitizing program computed the three-dimensional paths of the targets, allowing the three non-colinear targets of the hand to be linked together, and the three targets of the forearm to be linked together. Target linkages were necessary to perform the stick figure plots which will be discussed in the results section.

To edit the digitized tracking files, the three-dimensional track editor was used. This automatic program performed four automatic editing functions and provided 3-D paths to be edited in an interactive mode. The data editing

Table 1: Three-dimensional Position Data

PATH NUMBER	FRAME NUMBER	TIME seconds	X centimeter	Y centimeter	Z centimeter
Object Name : rtforearm					
1	1	0.	10.7625	15.5523	110.0684
1	2	0.167E-01	10.7625	15.5523	110.0684
1	3	0.333E-01	10.7408	15.5936	110.0694
1	4	0.500E-01	10.7543	15.5968	110.0850
1	5	0.667E-01	10.6885	15.6029	110.1471
1	6	0.833E-01	10.7066	15.6334	110.1502
1	7	0.100	10.7542	15.6218	110.1657
1	8	0.117	10.7542	15.6218	110.1657
1	9	0.133	10.7885	15.5859	110.1594
1	10	0.150	10.8127	15.5888	110.1622
1	11	0.167	10.8294	15.5525	110.1592
1	12	0.183	10.8247	15.5612	110.1591
1	13	0.200	10.8294	15.5525	110.1592
1	14	0.217	10.8294	15.5525	110.1592
1	15	0.233	10.8294	15.5525	110.1592
1	16	0.250	10.8294	15.5525	110.1592
1	17	0.267	10.8322	15.5351	110.1436
1	18	0.283	10.8322	15.5351	110.1436
1	19	0.300	10.8125	15.4944	110.1238
1	20	0.317	10.8533	15.5417	110.0965
1	21	0.333	10.8456	15.4887	110.1002
1	22	0.350	10.8577	15.4715	110.1201
1	23	0.367	10.8687	15.5076	110.1004
1	24	0.383	10.9108	15.4758	110.1296
1	25	0.400	10.9108	15.4758	110.1296
1	26	0.417	10.9918	15.4719	110.1031
1	27	0.433	10.9918	15.4719	110.1031
1	28	0.450	10.9918	15.4719	110.1031
1	29	0.467	10.9467	15.4230	110.1269
1	30	0.483	10.9611	15.3746	110.1129
1	31	0.500	10.9658	15.3629	110.1130
1	32	0.517	10.9658	15.3629	110.1130
1	33	0.533	10.9685	15.3155	110.0973
1	34	0.550	10.9497	15.3381	110.0779
1	35	0.567	10.9685	15.3155	110.0973
1	36	0.583	10.9428	15.3051	110.0638
1	37	0.600	10.9707	15.2981	110.0376
1	38	0.617	10.9500	15.2757	110.0486
1	39	0.633	10.9500	15.2757	110.0486
1	40	0.650	10.9500	15.2757	110.0486
1	41	0.667	10.9397	15.2645	110.0540
1	42	0.683	10.9397	15.2645	110.0540
1	43	0.700	10.9397	15.2645	110.0540

functions automatically performed were: elimination of all trajectories not associated with a named target, removal of all one-point paths (a one-point path has no slope and cannot be joined to other portions of the same path using cubic splines), interpolation over all gaps in each path using cubic splines, and removal of all beginning and end frames that did not contain a complete set a data (Motion Analysis Corporation, 1987). In the interactive editing mode, the tracked files were selectively cut and joined over specific time intervals where data were unavailable due to target cross-over or where system noise interferred with path curves.

A computer software program written to calculate Euler angles using the track-edited files will be found in Appendix I. The individual target path data from the track editor files were separated and the target paths were then split into x-axis, y-axis, and z-axis coordinate components in order to utilize the data to form two local coordinate systems. Unit vectors were formed from the separated three-dimensional position data.

The targets on the head of the third metatarsal and over the head of the capitate represented a proximal-distal axis which is commonly used by physical and occupational therapists to measure the range of motion of the wrist. The target on the head of the second metacarpal completed the triad of non-colinear points which formed the basis for the development of the local coordinate system of the hand

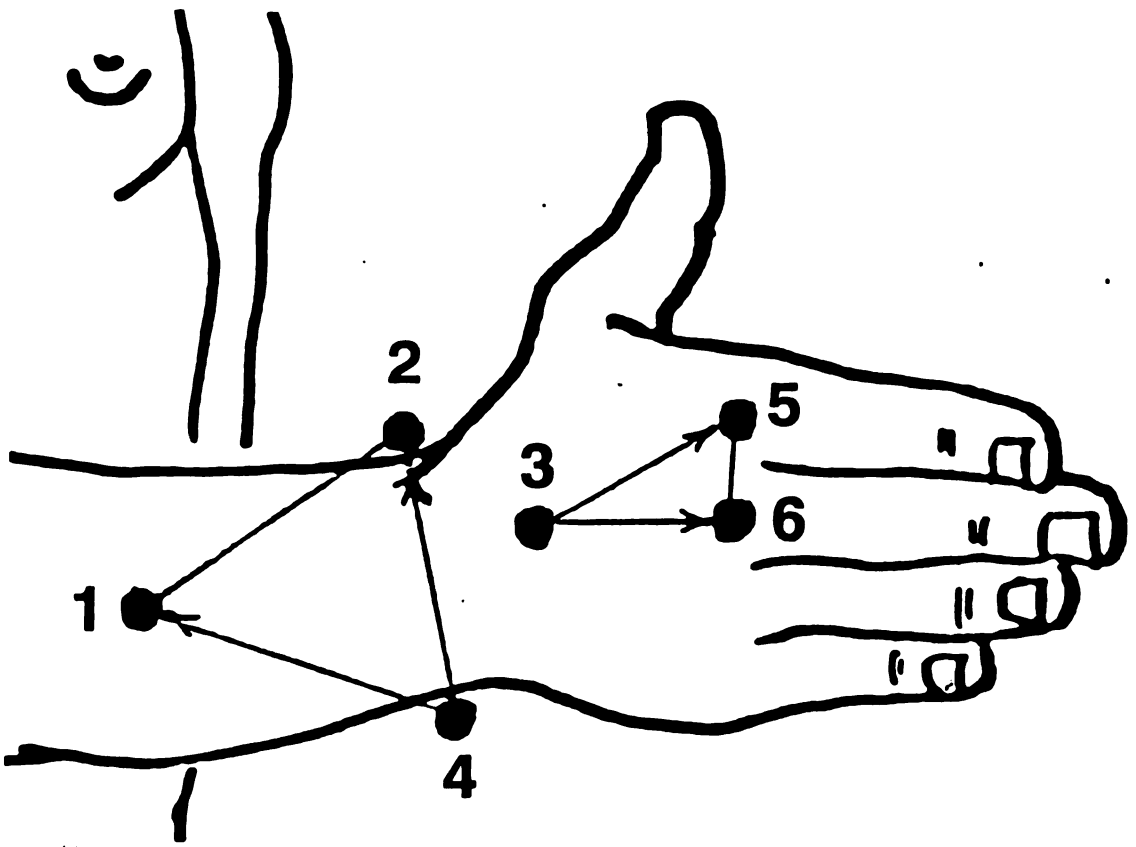

Figure 6: Wrist Triads

(see Figure 6). The forearm axis, usually determined to be a proximal-distal axis lying between the radius and ulna (bisecting the forearm) was not selected for the local coordinate system. Instead, an axis was formed between the radial and ulnar styloids (see Figure 6) because of the prominence of the bony styloids and the minimal skin motion which occurs over these landmarks. Soft-tissue motion causes distortion of data as skin motion will be falsely calculated as rigid body motion. A target on the dorsum of the forearm completed the triad of the forearm. The axes through the styloids and through the third metacarpal were approximately perpendicular.

The two local right-handed coordinate systems were formed with the origin of the hand segment coordinate system at the target over the head of the capitate and the forearm segment coordinate system over the ulnar styloid. The following vector formulas were used in the calculations of these coordinate systems:

$$\vec{36} = \vec{P6} - \vec{P3} \qquad \vec{42} = \vec{P2} - \vec{P4} \qquad (1)$$

$$\vec{35} = \vec{P5} - \vec{P3} \qquad \vec{41} = \vec{P1} - \vec{P4}$$

$$\hat{Hy} = \vec{36} / [\vec{36}] \qquad \hat{Fz} = \vec{42} / [\vec{42}] \qquad (2)$$

$$\hat{Hx} = \vec{36}\vec{X}\vec{35} / [\vec{35}\vec{X}\vec{36}] \qquad \hat{Fx} = \vec{42}\vec{X}\vec{41} / [\vec{42}\vec{X}\vec{41}] \qquad (3)$$

$$\hat{Hz} = \hat{Hx} \; X \; \hat{Hy} \qquad \hat{Fy} = \hat{Fz} \; X \; \hat{Fx} \qquad (4)$$

where: $\vec{Pn}$ is the position data for target n.

$\hat{Hx}$, $\hat{Hy}$, $\hat{Hz}$ are the unit vectors for the hand coordinate system.

$\vec{A} \times \vec{B}$ is the cross product of A cross B

$\hat{Fx}$, $\hat{Fy}$, $\hat{Fz}$ are the unit vectors for the forearm coordinate system.

$$[\vec{AB}] = \sqrt{(Bx - Ax)^2 + (By - Ay)^2 + (Bz - Az)^2}$$

The above formulas defined the formation of unit vectors perpendicular to the dorsal body segments from the cross-products of the vectors created on the segment surface. The third orthogonal coordinate vectors of the two local segment coordinate systems were formed by the cross products of the third metacarpal axis with the perpendicular dorsal vector and by the cross product of the styloid axis with the perpendicular vector formed there.

A joint coordinate system having unit base vectors denoted $\hat{e}_1$, $\hat{e}_2$, and $\hat{e}_3$ suggested by Grood and Suntay (1983) was formed. An illustration of unit vectors is found in Figure 7. The unit coordinate vector $\hat{e}_1$ was selected to coincide with the $\hat{Hx}$-axis of the hand (H = hand). The $\hat{e}_3$ unit coordinate vector was chosen to coincide with the $\hat{Fz}$-axis of the forearm (F = forearm). A third non-orthogonal unit coordinate vector (also called the "floating axis")

which is mutually perpendicular to and formed from the cross product of the other two unit coordinate vectors (see Figure 7) was calculated as follows:

$$\hat{e}_1 = \hat{H}x \qquad (5)$$

$$\hat{e}_3 = \hat{F}z \qquad (6)$$

$$\hat{e}_2 = \hat{e}_3 \times e_1 \,/\, [\hat{e}_3 \times \hat{e}_1] \qquad (7)$$

where: $[\hat{e}_3 \times \hat{e}_1] =$

$$\sqrt{(\hat{e}_3 y \hat{e}_1 z - \hat{e}_3 z \hat{e}_1 y) + (\hat{e}_3 z \hat{e}_1 x - \hat{e}_3 x \hat{e}_1 z) + (\hat{e}_3 x \hat{e}_1 y - \hat{e}_3 y \hat{e}_1 x)}$$

Rotations about the floating axis $\hat{e}_2$ were reported as supination and pronation although this definition is a misnomer. Traditionally, pronation and supination are defined as movements of the forearm about its longitudinal axis. This rotatory movement of the forearm involves the mechanically linked superior and inferior radio-ulnar joints and not the radiocarpal or midcarpal joints of the wrist. For simplicity, the designations of supination and pronation were used because they are familiar to all clinicians. With the elbow flexed at 90 degrees and the thumb pointing superiorly, a supinating rotation was defined as rotating the palm to face superiorly and the thumb to point laterally (Kapandji, 1985) (see Figure 8a). A pronating rotation caused the palm to face inferiorly and the thumb to point medially (see Figure 8b).

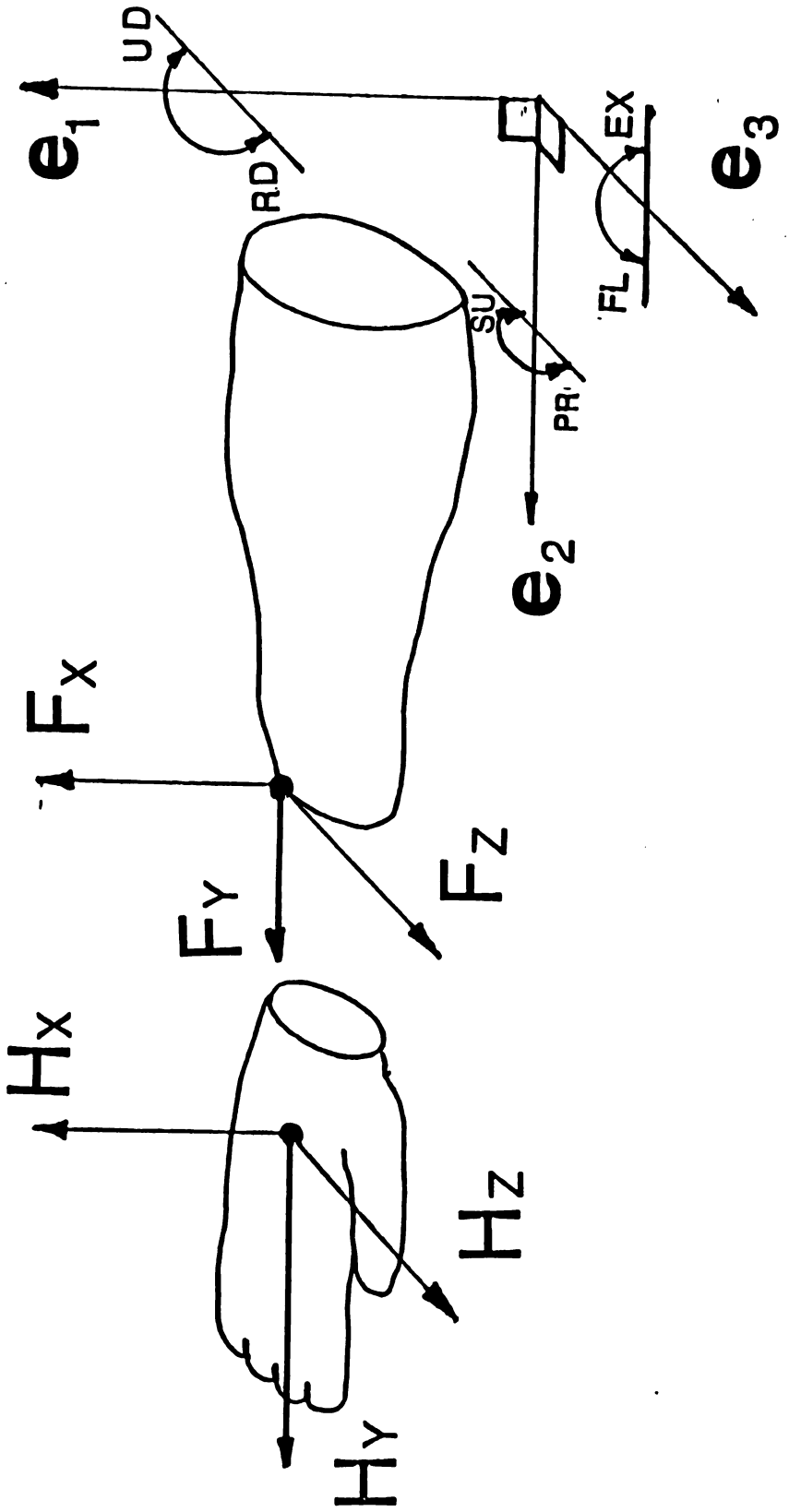

Figure 7: Non-orthogonal Coordinate System

a. supination b. pronation

Figure 8: Supination and Pronation

Construction of the non-orthogonal joint coordinate system allowed three independent Euler angles to be calculated from the dot products (projections) between the two local segment and the joint coordinate system. Since the joint coordinate system remains on the body segments during motion, the joint angles could be calculated independent of the order of rotation. The following equations were used for angle calculations:

$$\text{Ulnar}(+) \text{ and radial}(-) \text{ deviation} = \sin^{-1}(\hat{Hz} * \hat{e}_2) \quad (8)$$

$$\text{Extension}(+) \text{ and flexion}(-) = \sin^{-1}(\hat{Fx} * \hat{e}_2) \quad (9)$$

$$\text{Pronation}(+) \text{ and supination}(-) = \sin^{-1} (\hat{e}_3 * \hat{e}_1) \quad (10)$$

where: * is the dot product sign

For an illustration of the vectors used in these dot product equations, refer to Figure 7.

The Expertvision software provided a smoothing operator which took a weighted average of thirteen points for computation of the centroid thus forming a thirteen point window. This program removed angle path spikes by averaging the data over a group of data. Hence, the greater the window value, the smoother the path. This smoothing program acted as a low-pass filter that supressed localized deviations without substantially changing the overall form of path and time series data. A thirteen point window was chosen because, according to Mann et al.(1989), 75% of the spectral energy of the wrist occured at less than five hertz. Since the data were collected at 60 frames per second, normal wrist motion will occur every twelveth frame. The computer software accepted only odd numbers for window width and thus a thirteen point window was chosen.

RESULTS

To adequately evaluate the motions of the human wrist, two computer software programs were utilized. The first utilized the motion analysis software package which provided a three-dimensional stick-figure software graphics operator. The stick command produced six different orthogonal views of the stick figure data where the images were projected onto the view plane using an orthographic projection (Motion Analysis Corporation, 1987). The superimposed stick figure tracings and the target path trajectories of a particular wrist motion provided a graphical model for analysis. An example of superimposing the full 300 frames of the file containing wrist circumduction motion is illustrated in Figure 9, while the model in Figure 10 has every tenth frame superimposed. Superimposed tracings may also be divided into different time increments throughout the motion cycle to improve visualization of motion irregularities. The stick figure program also allowed the baseline to be labeled in frames, in percentage of the time interval, or in time units. Stick figure graphics from the position data of circumduction, flexion/extension, and radial/ulnar deviation motions illustrated in Figures 11, 12, and 13 respectively, were plotted by percentage of time. Note that the second

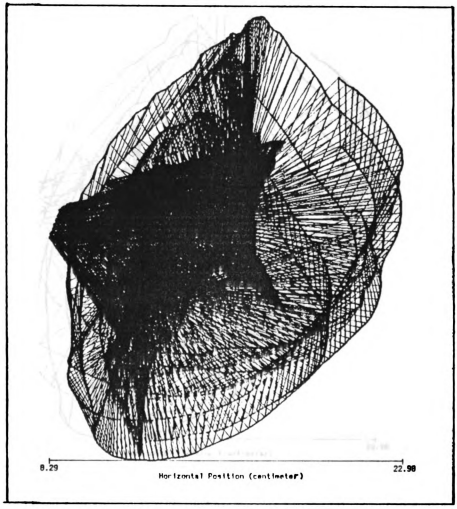

Figure 9: Superimposed Tracings of all Frames of Circumduction (Trial 1)

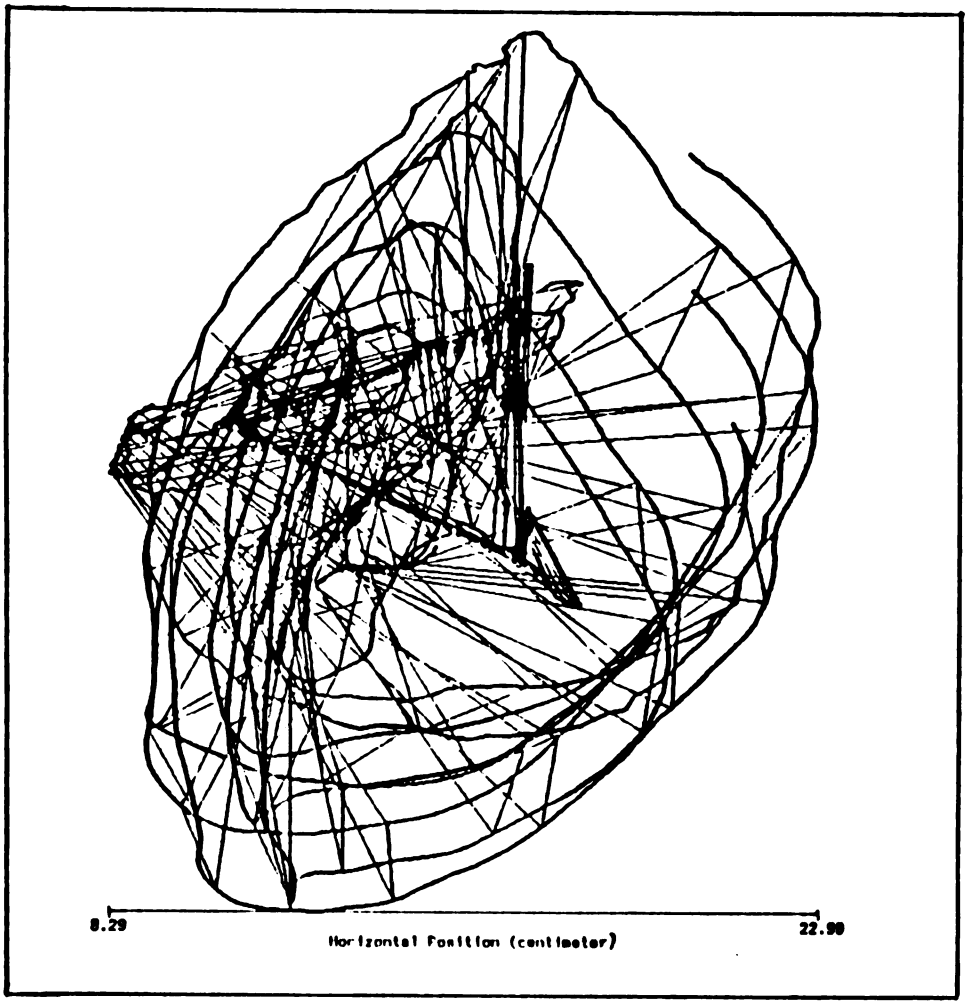

Figure 10: Superimposed Tracings of Every Tenth Frame of Circumduction (Trial 1)

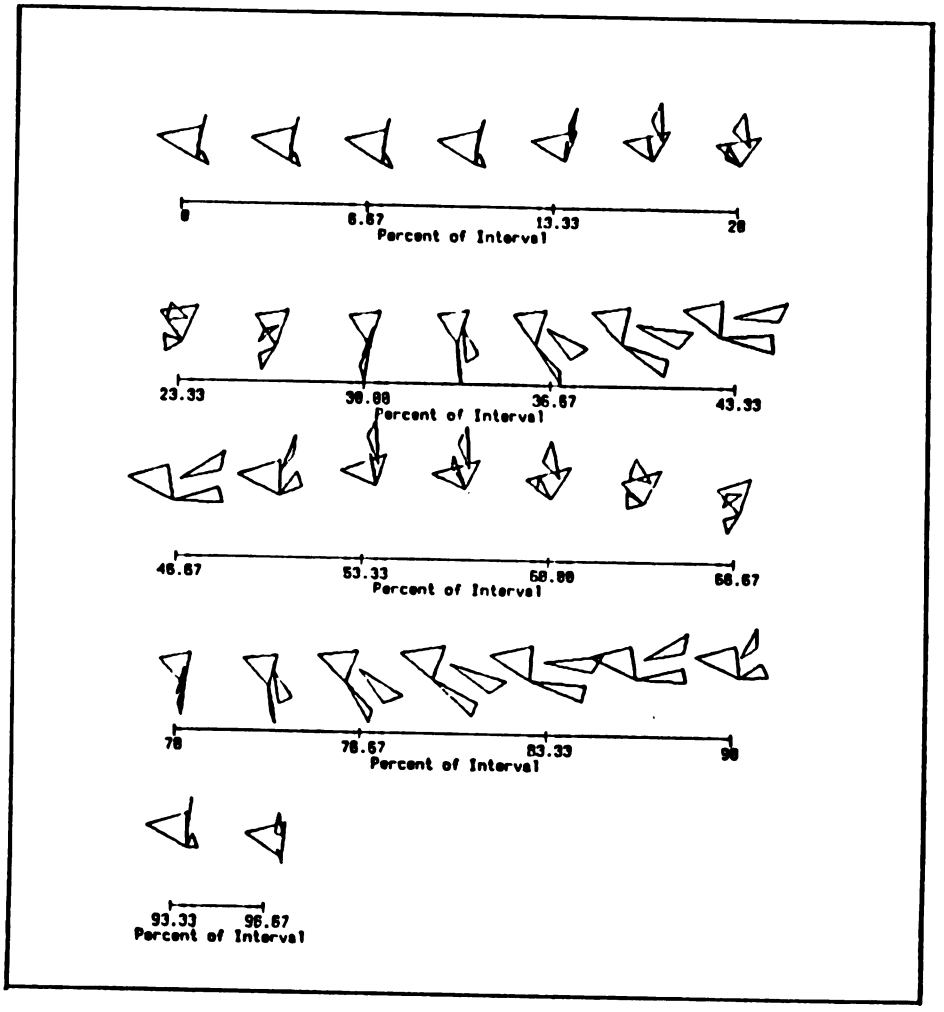

Figure 11: Circumduction Position Data By Percentage of Time Interval

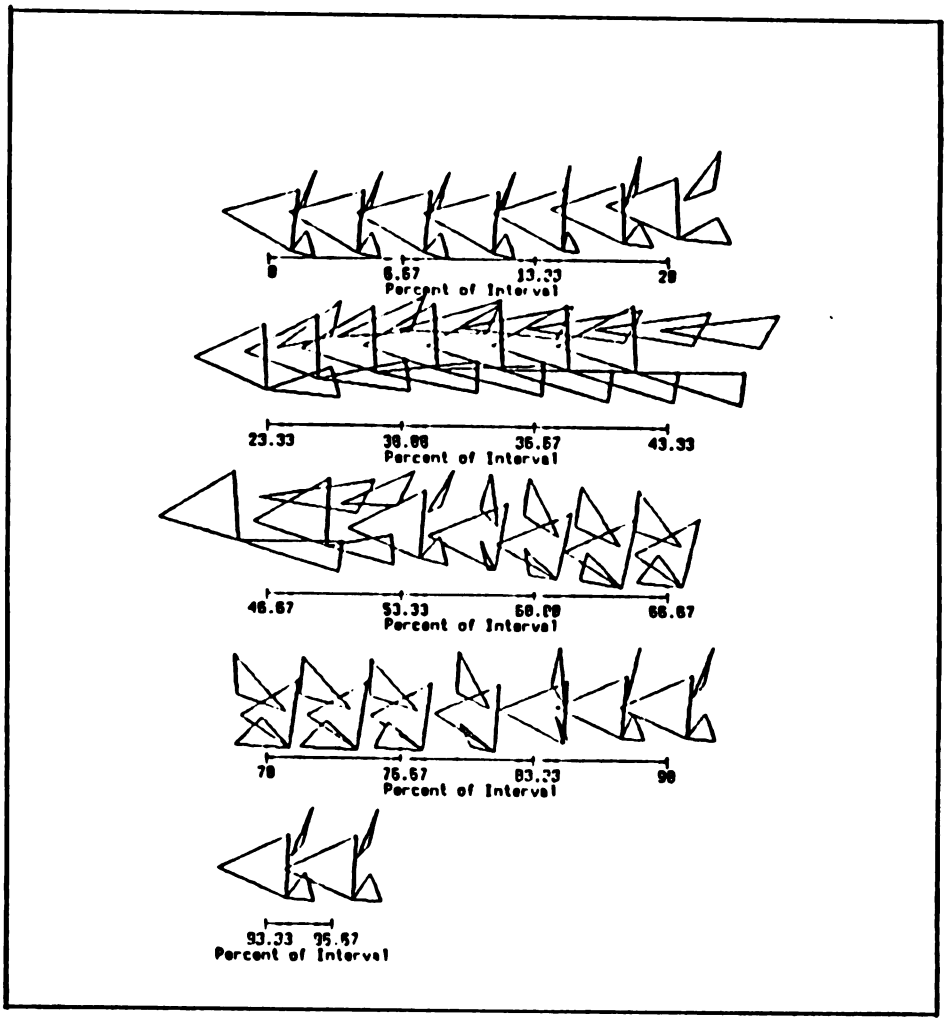

Figure 12: Flexion/Extension Position Data By Percentage of Time Interval

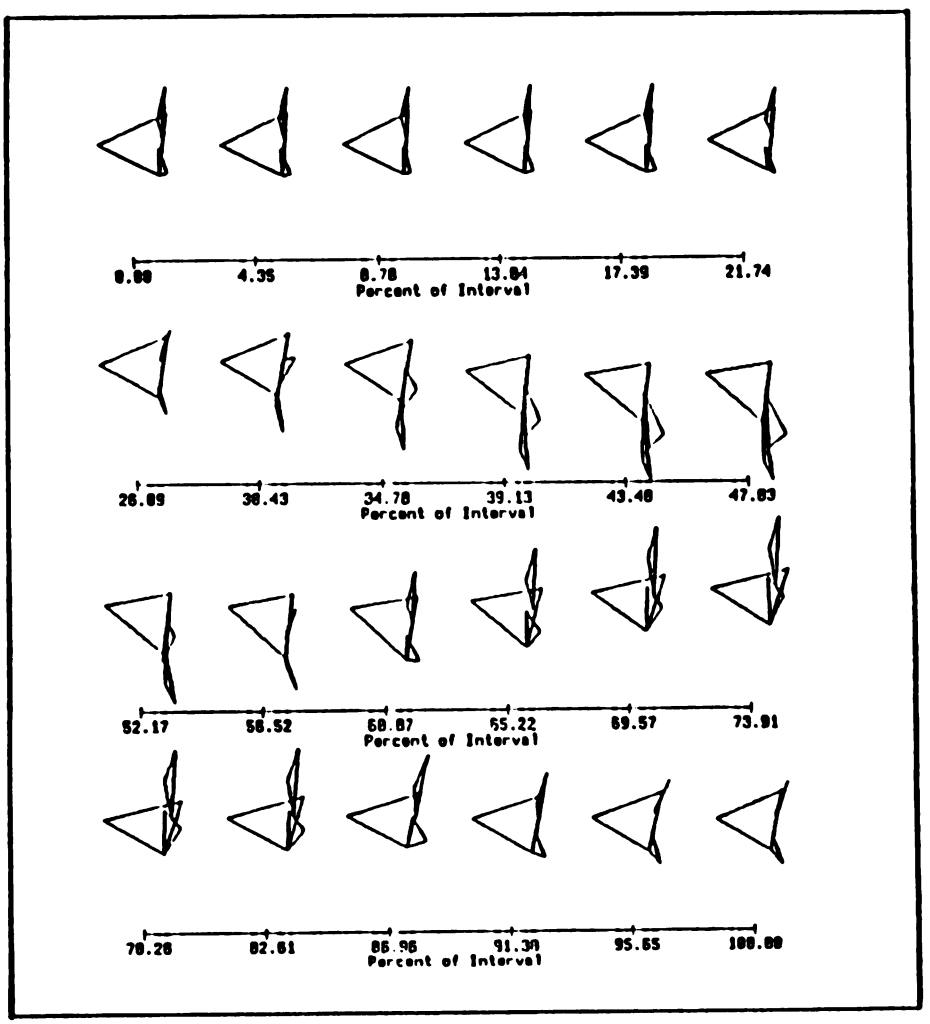

Figure 13: Radial/Ulnar Deviation Position Data By Percentage of Time Interval

triad shown on the hand segments of Figures 11, 12, and 13 was a separate triad formed between the targets on the ulnar styloid and the fourth and fifth metacarpal heads. The triad formed by these markers was not included in the analysis of the joint coordinate system (see Figure 14).

The joint coordinate system provided joint angle plots against a baseline of time (sec). Rotations about the three coordinate axes ($\hat{e}_1$, $\hat{e}_2$, and $\hat{e}_3$) for the track edited data are shown in Figures 15 through 20. Horizontal plots seen at the beginning of each curve in each of these six figures, indicate a "comfortable" position from which the actions of

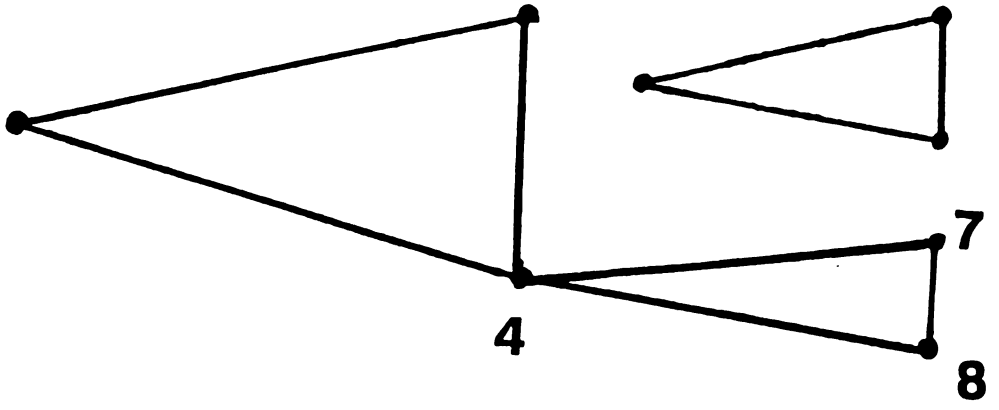

Figure 14: Accessory Hand Triad (4-7-8)

the wrist occurred. Plottings above the neutral joint angles represent extension (EX), ulnar deviation (UD), and pronation (PR) motions of the wrist. Plottings below the neutral joint angles represent flexion (FL), radial deviation (RD), and supination (SU) motions of the wrist. Neutral joint angles were calculated from position data of wrist held in a neutral position. The estimated neutral joint angles about the three non-orthogonal axes are illustrated by horizontal lines in Figure 21.

Path and time series plots of rotations about the individual axes allowed for closer examination of the curves as illustrated in Figures 22 through 24 for circumduction. Circumduction was divided into its components of flexion-extension, radial-ulnar deviation, and supination-pronation.

To calculate the ROM about an axis in a single direction, the neutral joint angle had to be estimated from a neutral position trial. The estimated average of the neutral joint angles about the three non-orthogonal axes are illustrated in Figure 23.

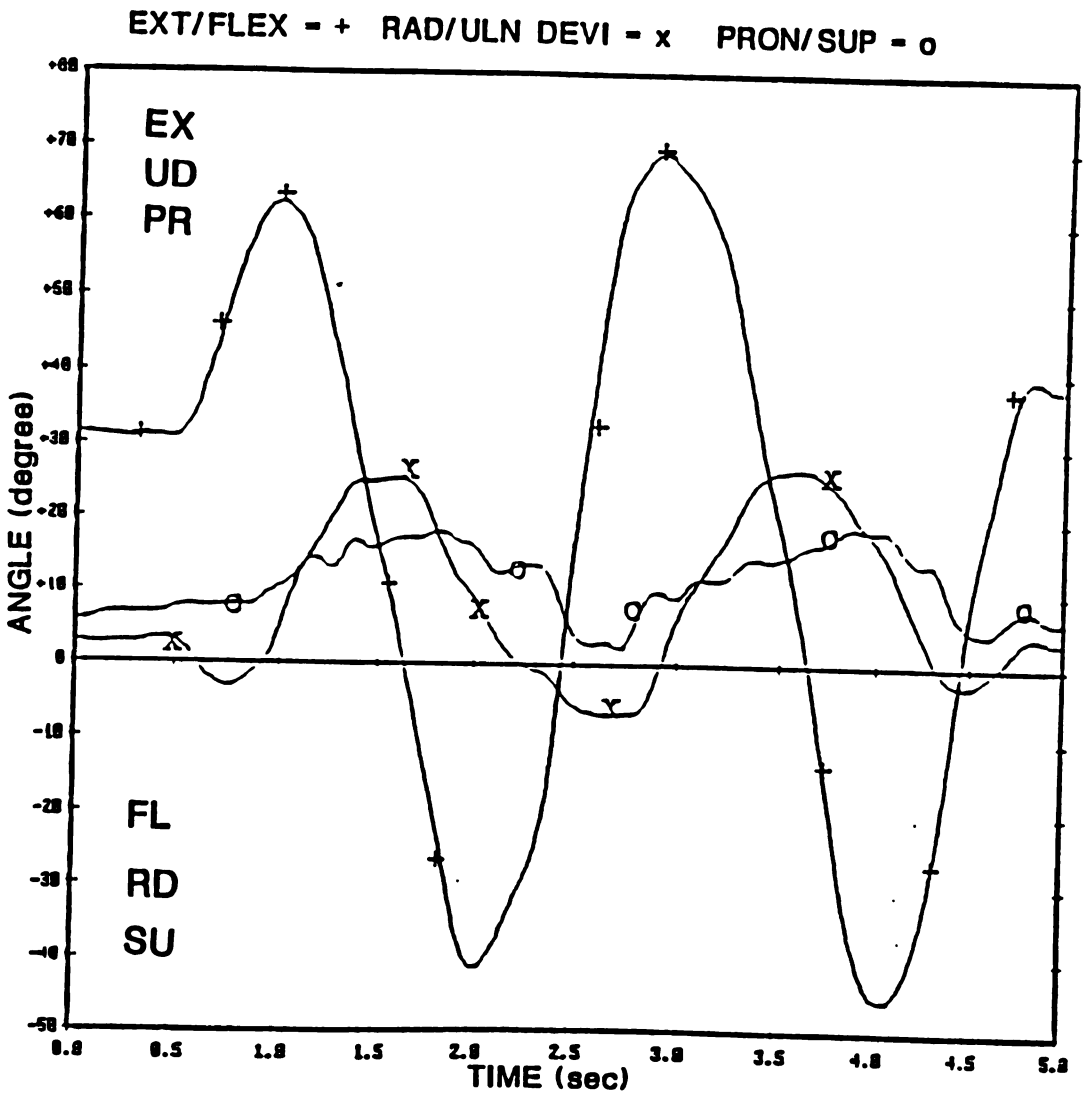

Figure 15: Angle Displacement Plots for Circumduction (Trial 1)

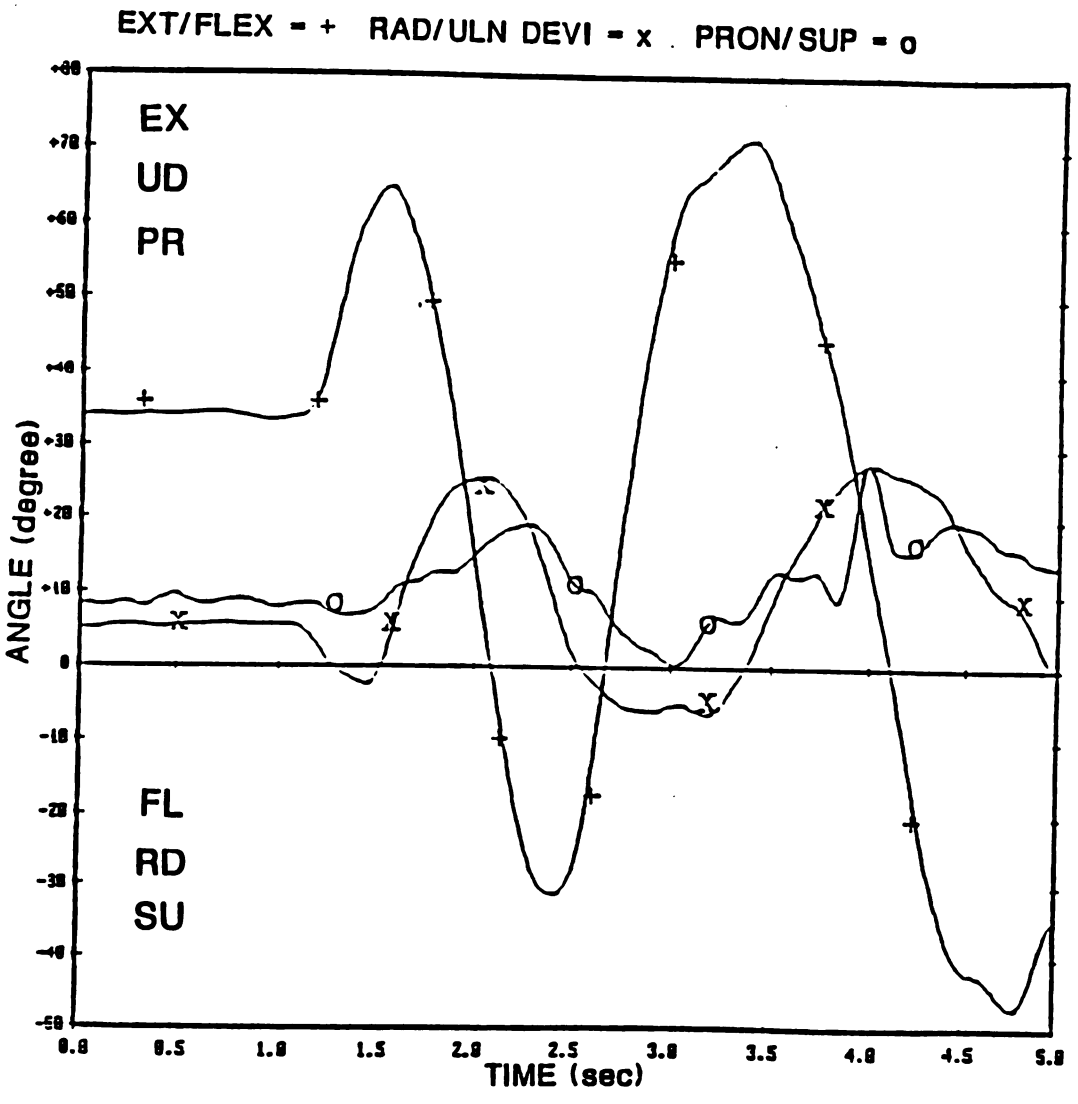

Figure 16: Angle Displacement Plots for Circumduction (Trial 2)

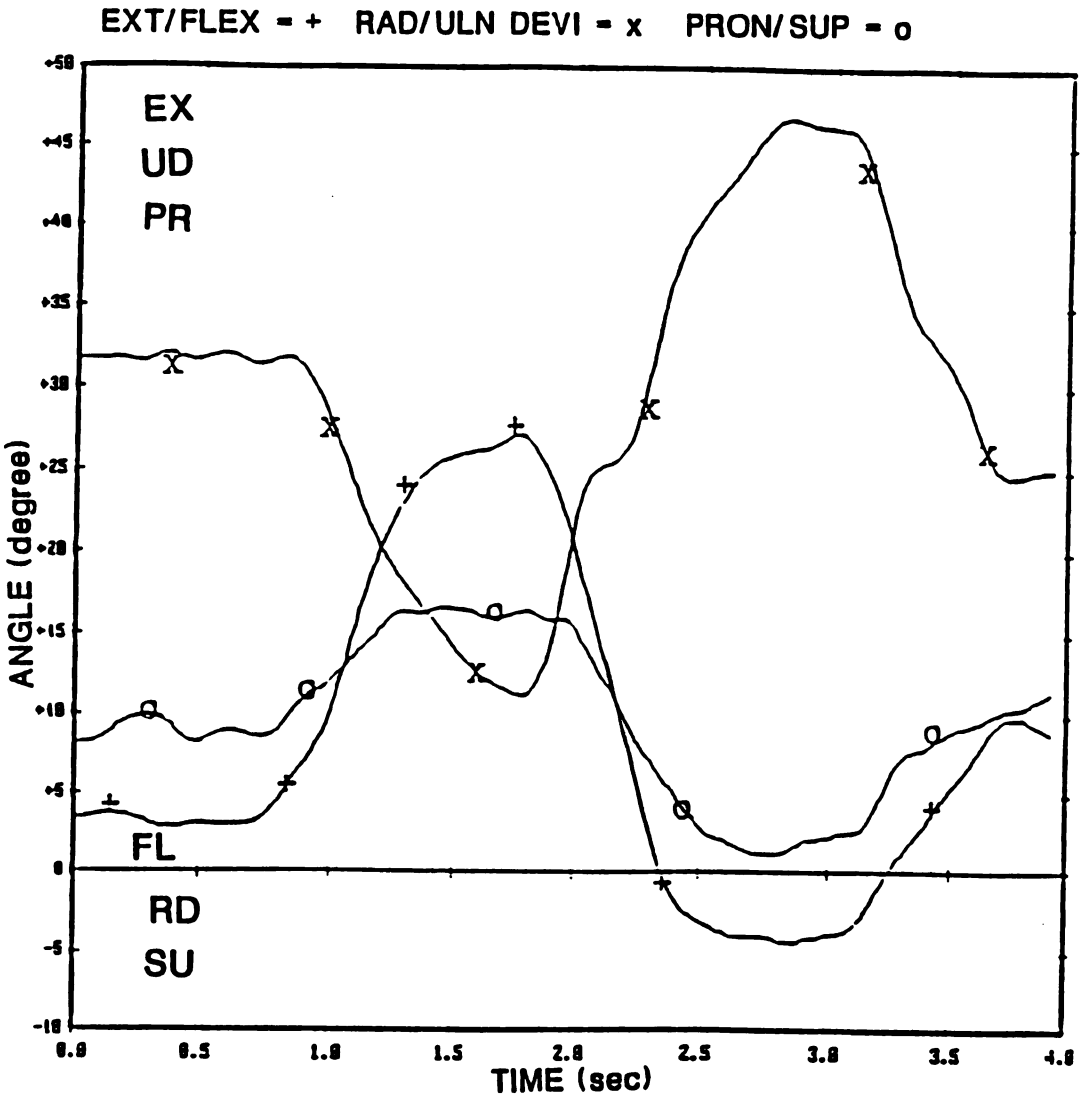

Figure 17: Angle Displacement Plots for Flexion/Extension (Trial 1)

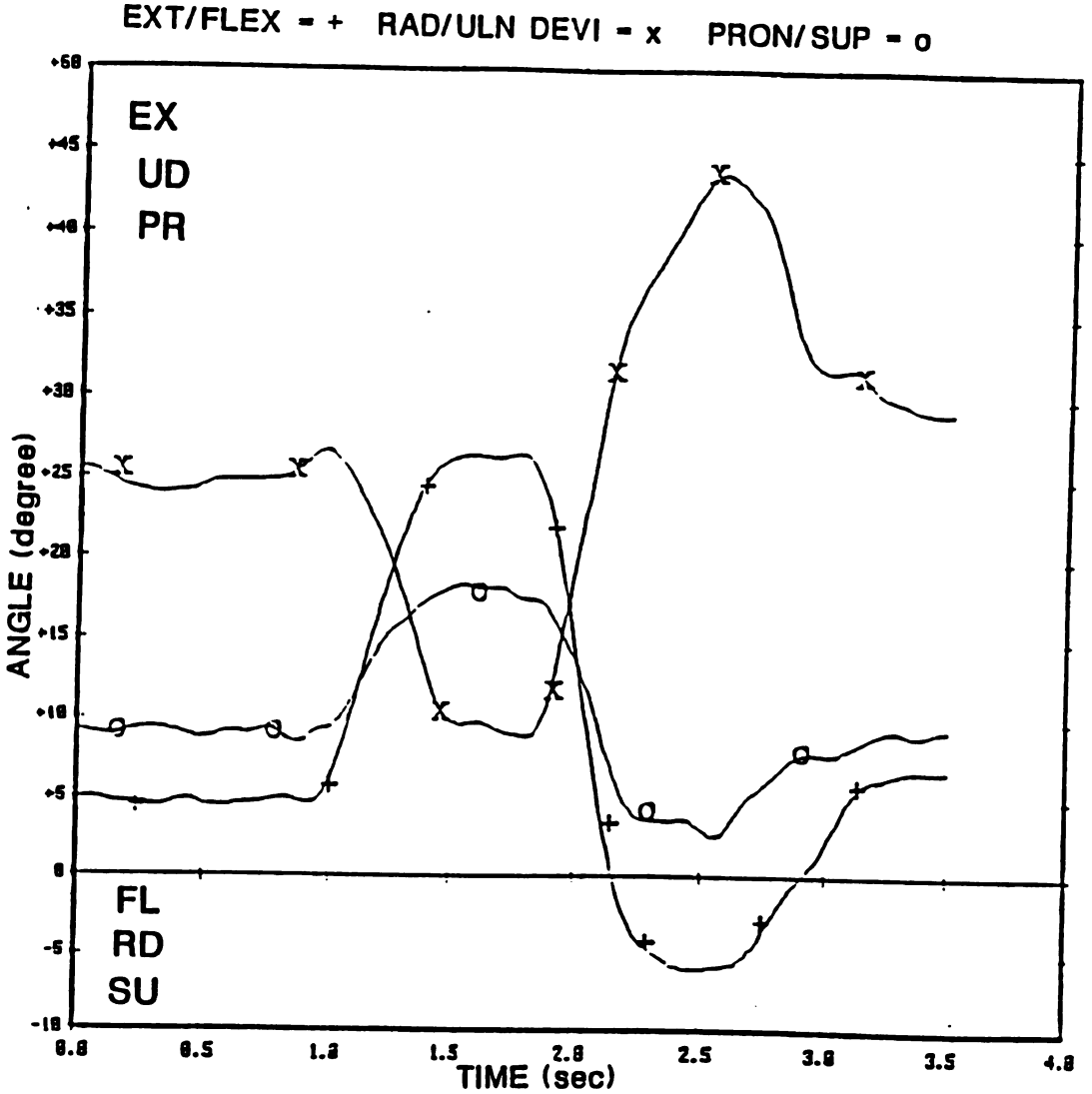

Figure 18: Angle Displacement Plots for Flexion/Extension (Trial2)

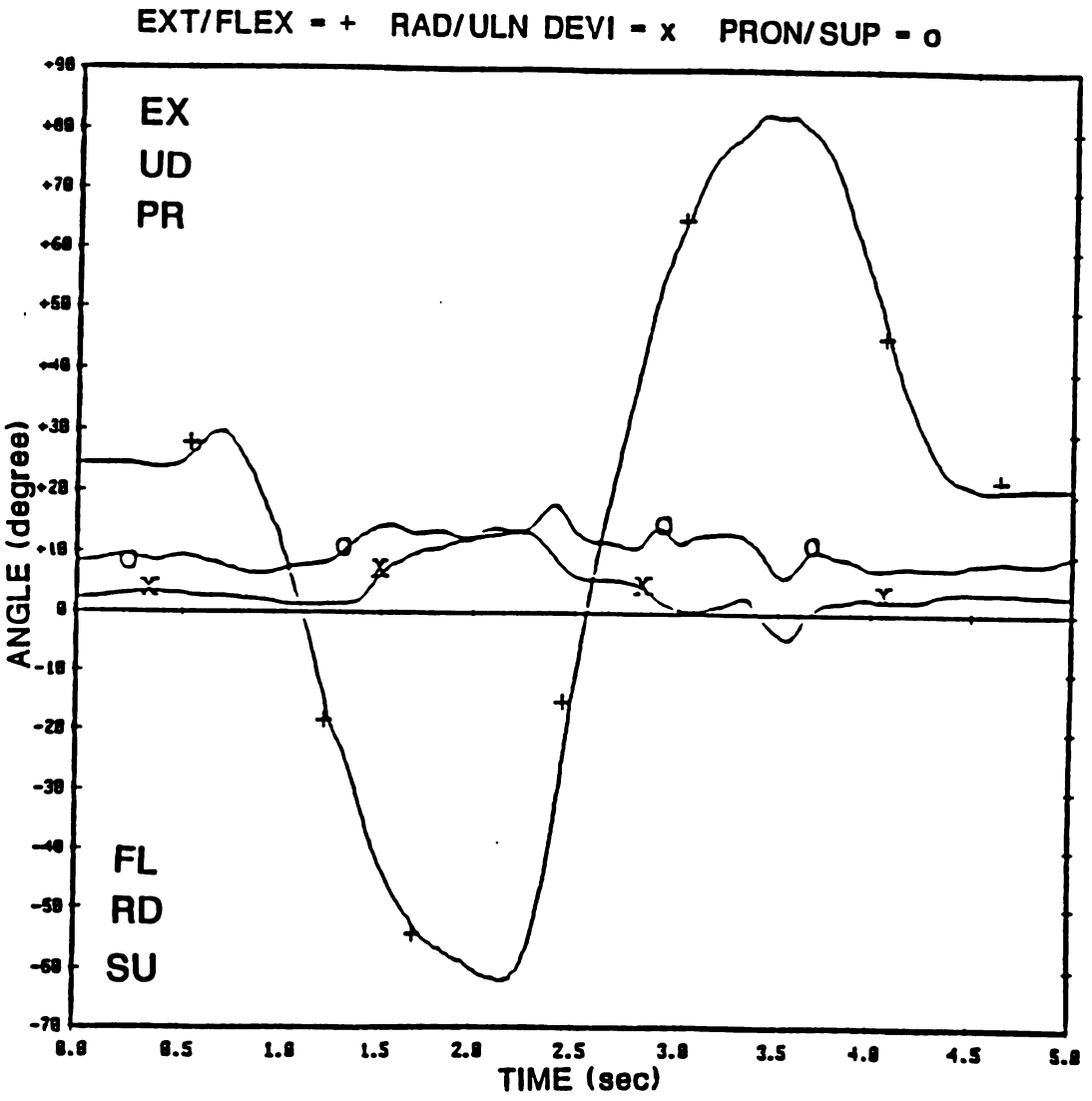

Figure 19: Angle Displacement Plots for Radial/Ulnar Deviation (Trial 1)

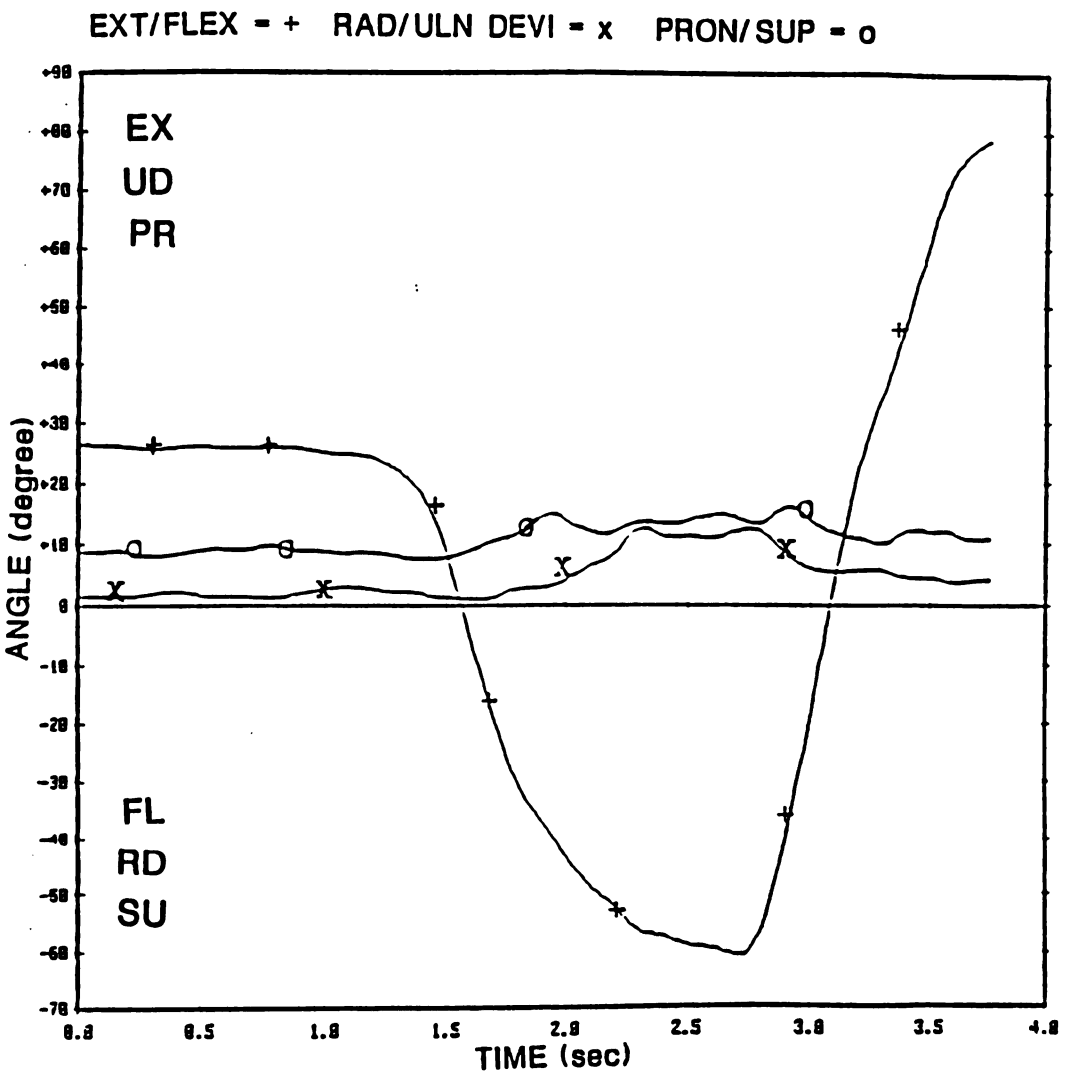

Figure 20: Angle Displacement Plots for Radial/Ulnar Deviation (Trial 2)

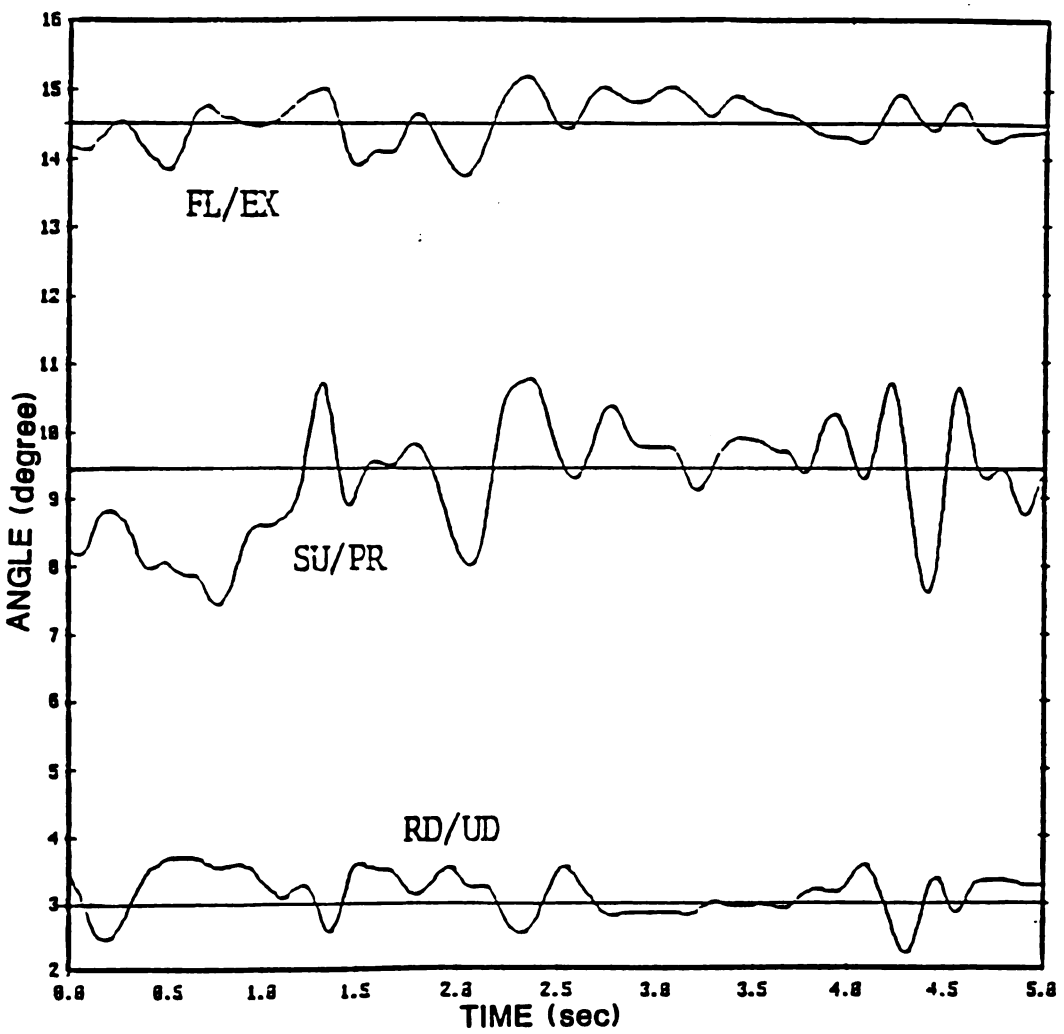

Figure 21: Neutral Joint Angle Plots

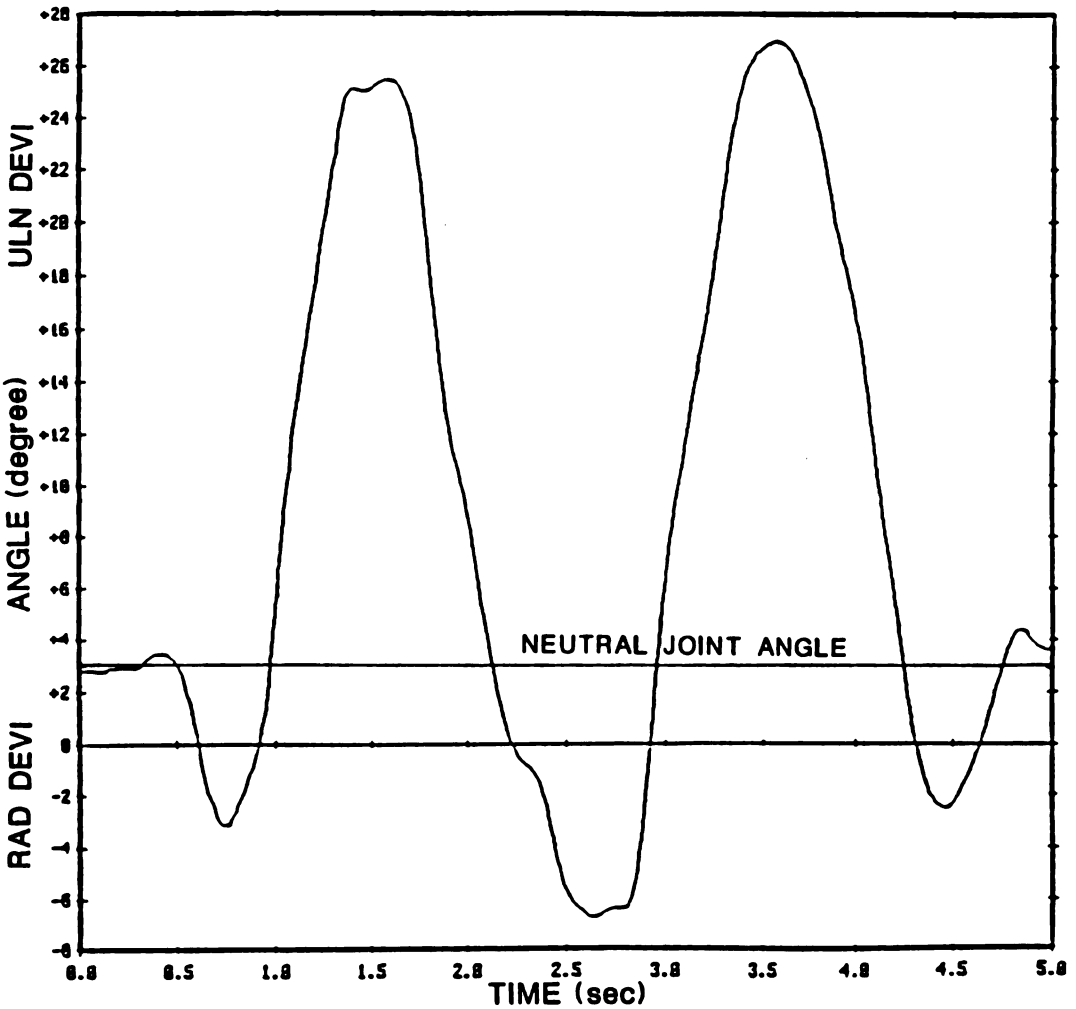

Figure 22: Flexion-extension Displacement Angle Plot for Circumduction (Trial 1)

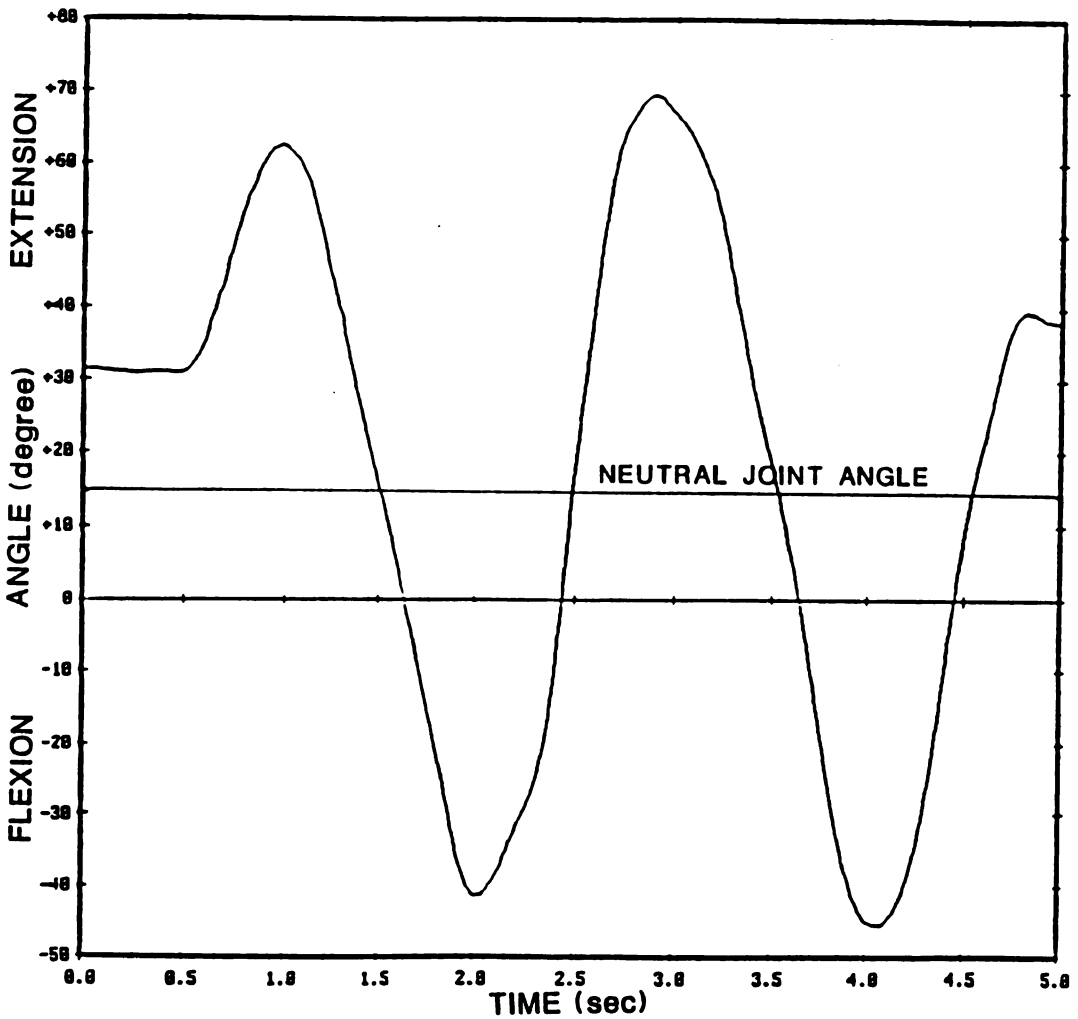

Figure 23: Radial-ulnar Deviation Displacement Angle Plot for Circumduction (Trial 1)

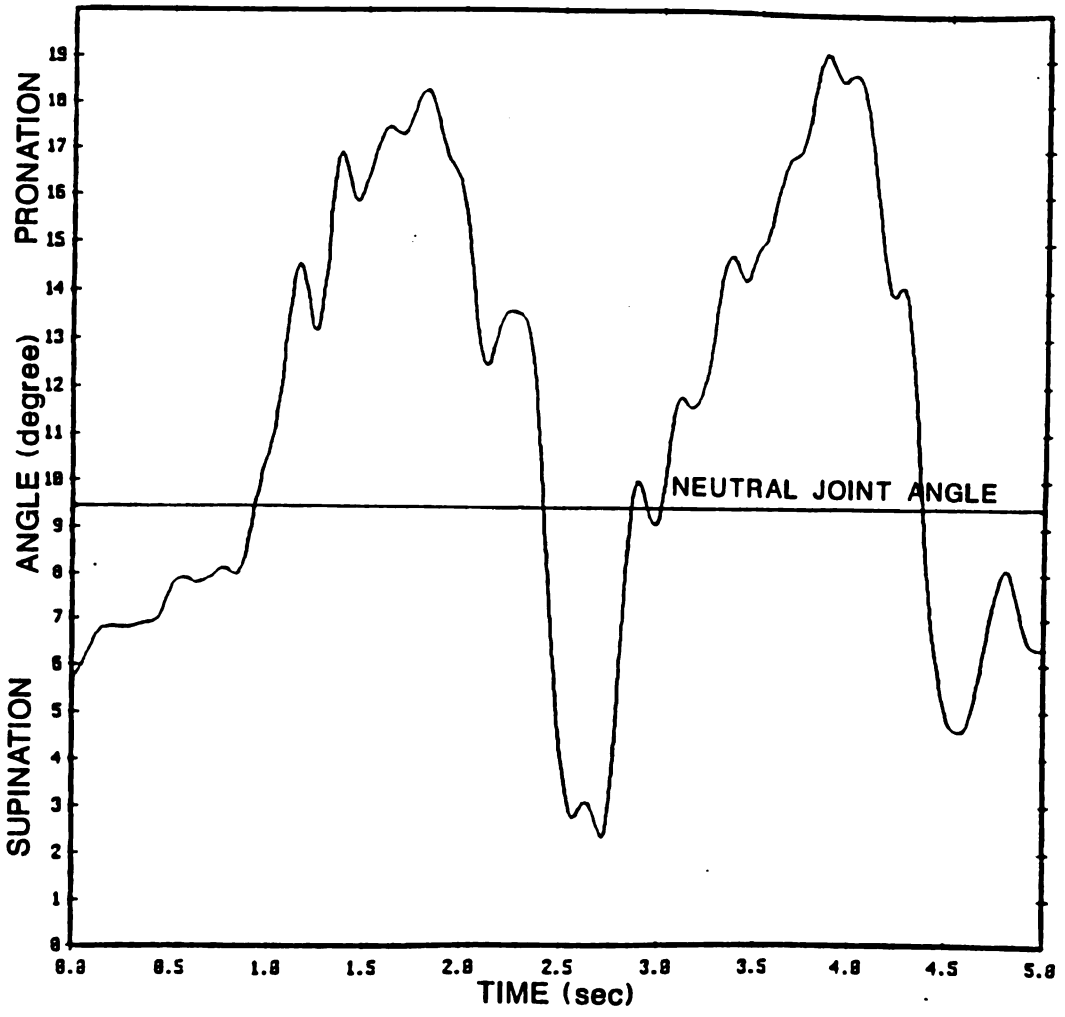

Figure 24: Supination-pronation Displacement Angle Plot for Circumduction (Trial 1)

DISCUSSION

The joint coordinate data analysis will be discussed in the following section. In addition, the active ranges of motion calculated about the Euler angles will be compared with the values found in previous studies.

The vertical line in the initial portions of data paths of the Figures 15 through 23 was indicative of a resting joint position (ie: the wrist was resting in a relaxed position during this time phase). Note that the resting joint position and the neutral joint angle were not equal for all trials.

The motion sequence for circumduction was: extension, ulnar deviation, flexion, and radial deviation. Pronation of the wrist followed the ulnar deviation motions of the wrist. The total rotation or range of motion about the three coordinate axes for the two circumduction motion files is found in Table 2.

In performing a relatively planar flexion motion with the wrist, the subject increased rotation about the $\hat{e}_3$ axis from 114.97 and 118.65 degrees during circumduction motions to 144.72 degress during planar flexion, or approximately 24% during flexion-extension motion (trial 1). Note that the rotations about the other two coordinate axes $\hat{e}_1$ and $\hat{e}_2$

Table 2: Active Range of Motion of Three Degree-of-Freedom Wrist Model

ANGLE RANGE / MOTION PERFORMED	FLEXION *	EXTENSION *	TOTAL FLEXION-EXTENSION	RADIAL DEVIATION *	ULNAR DEVIATION *	TOTAL RAD/ULN DEVIATION	SUPINATION *	PRONATION *	TOTAL SUPINATION-PRONATION
CIRCUMDUCTION (TRIAL 1)	60.0	54.97	114.97	9.70	23.98	33.68	6.23	9.21	15.44
CIRCUMDUCTION (TRIAL 2)	61.56	57.09	118.65	9.23	24.95	34.18	7.78	11.67	19.45
FLEXION-EXTENSION (TRIAL 1)	76.45	68.27	144.72	7.35	10.51	17.86	2.56	6.25	8.81
# FLEXION-EXTENSION (TRIAL 2)	75.25	64.37	139.62	1.95	9.63	11.58	1.64	5.24	6.88
RADIAL-ULNAR DEVIATION (TRIAL 1)	3.30	32.30	35.60	7.37	24.21	31.58	7.90	7.07	14.97
RADIAL-ULNAR DEVIATION (TRIAL 2)	5.56	29.24	34.80	9.0	23.48	32.48	6.05	8.77	14.82
NEUTRAL JOINT ANGLE	14.50			3.00			9.40		

* individual motion ranges calculated as maximum displacement angle minus neutral joint angle

\# angle displacement plots for this trial do not contain a complete cycle of flexion-extension

of the flexion-extension trial were relatively small (17.86 and 8.81 degrees respectively) in comparison to the circumduction trials (approximately 34 and 17 degrees respectively). The path data for flexion (trial 2) was prematurely ended due to target merging during target tracking. Consequently, only 3.75 seconds of data for flexion (trial 2) were available for processing. Therefore, the ROM values for this file in Table 2 do not contain a full cycle of wrist flexion-extension motion.

Figures 18 and 19, representing the rotations about the three coordinate axes for the two actions of radial-ulnar deviation of the wrist were similar. Although these files encompassed only 3.5 and 3.9 seconds of data, a full cycle of ulnar to radial deviation was captured for each trial. During ulnar deviation of the wrist, large flexion and pronation components were occuring simultaneously. With radial deviation, components of extension and supination also were present. It was apparent that the subject was unable to restrain the wrist motion to a single plane. This information is consistent with current knowledge that joint motion is coupled. Note that radial-ulnar deviation of the wrist did not substantially change the total radial-ulnar deviation range of motion (31.58 and 32.48 degrees) in comparison to the total radial-ulnar deviation angle range during circumduction of the wrist (33.68 and 34.18 degrees).

Previous authors reported a wide range of values for the normal ROM's of the wrist. The values for the

Table 3: Previously Reported Ranges of Motion

ANGLE RANGE / AUTHOR(S)	FLEXION	EXTENSION	TOTAL FLEX/EXT	RADIAL DEVIATION	ULNAR DEVIATION	TOTAL RAD/ULN DEVIATION
DEBRUNNER (1982)	50-60°	35-60°	85-120°	25-30°	30-40°	55-70°
HECK (1965)	80°	70°	150°	20°	30°	50°
HOPPENFELD (1976)	80°	70°	150°	20°	30°	50°
KAPANDJI (1985)	85°	85°	170°	15°	30-45°	45-60°
POLLEY & HUNTER (1978)	80-90°	70°	150-160°	20°	50-60°	70-80°
VOLZ (1980)	66°	55°	121°	NA	NA	NA

individual motions of flexion, extension, radial deviation, and ulnar deviation and for the total range about each axes is shown in Table 3. The total range for flexion-extension motion of the wrist varied from 121 to 170 degrees. The total range for radial-ulnar deviation motion of the wrist varied from 45 to 80 degrees. The maximum values for flexion-extension and radial-ulnar deviation of the wrist in this study were 144.72 and 34.18 degrees respectively. Further comparisons can not be made, as this study analyzed only active (voluntary) range of motion while several of the authors in Table 3 analyzed passive range of motion.

Analysis of the data with the joint coordinate system revealed that rotation occurred about all three coordinate axes for the complex motions of circumduction, as well as for the simple motions of flexion-extension and radial-ulnar deviation.

CONCLUSIONS

In conclusion, the purpose of this study was to provide a methodology for the recording and analyzing of three-dimensional wrist motion using a three degrees-of-freedom model of the wrist. Analysis of the data revealed that rotation occurred about all three of the axes of the joint coordinate system for the three different wrist motions examined. The Sun-4 Motion Analysis System provided quick and accurate data collection for analysis of the rotations about the joint coordinate axes.

The general pattern of the curves for angular displacement of the joint coordinate axes was a model for each particular motion made by the wrist. The images created by the stick figure software program provide a tool to aid in the visualization of the motion of the hand and forearm. The final shape of the superimposed tracings of the stick figures could be compared to the stick figures of similar motions to assess motion irregularities.

Clinical applications of the knowledge gained with this methodology for analyzing human wrist motions are found in such fields as bioengineering, orthopaedics, prosthetics and orthotics. For physical and occupational therapists

involved with upper extremity rehabilitation, this methodology may be a valuable tool.

Knowledge of wrist kinematics pre and post surgery will enable the therapist to objectively document the changes that have occurred in the quantity and quality of motion. In cases where patients suffer from carpal tunnel syndrome where there is a narrowing of the ventral canal space through which the nerves, arteries, and tendons traverse and resection of the flexor retinaculum is necessary, therapists and physicians should be aware of the possible disruption in wrist kinematics. When assessing the kinematics of the wrist post-casting for four to eight weeks, caregivers also need to be aware of the changes that occur in the quality of motion secondary to static positioning over an extended period of time.

As medical insurance companies are requiring more extensive documentation on the progress of treatment, the evaluative tools used by the therapist become more complex. Measurement of the ROM of affected body segment and adjacent segments is commonly accomplished with the aid of a goniometer. The goniometer is a tool for acquisition of quick, gross measurement of the range of movement about an estimated axis of rotation in an estimated plane of motion. Therapists agree that ROM measurements of a patient will vary from one therapist to another or from day to day by the same therapist. The methodology described in this paper could provide an accurate tool for objective correspondance

between therapist, physician, and medical insurance company. Data acquisition and analysis could be completed within several hours, depending of the complexity of the motions analyzed. This could be a valued addition to a patients' report if the processing of data is cost effective.

A limitation of the study was the issue of skin motion, which must be addressed as a source of possible error in the data. Skin motion and the presence of subcutaneous adipose tissue are relatively minimized when targets are placed over a bony prominence. Skin motion may account for the noise in the plots for angular displacement of the joint coordinate system analysis. The paths could have been legitimately smoothed with a larger point window but until further studies are completed, true data loss with excessive smoothing can not be assessed.

Suggestions for Future Studies

In the field of prosthetics, as the science of total joint replacement advances, the aim of the orthopaedic surgeon and the prosthetist is to restore as much function to the affected extremity as possible. Prosthetists are already utilizing gait (motion) and force plate analysis to assist them in the design and adjustment of alignment of lower limb prosthetics. In the future, a functional, automated prosthetic upper extremity may need these same adjustments. Researchers have already used motion analysis to evaluate the kinematics of the wrist comparing

commercially available prosthetic wrist joints (Tolbert et al., 1985).

The plots of angular displacement may be used as models of human wrist motion. Future studies should compare these angular patterns for different functional activities. Comparisons may be made bilaterally between the wrists to compare the kinematics of the affected versus the unaffected wrist joint. Abnormalities and spikes in the motion curves may be indicative of joint pain or pathology during a particular range in the motion or during a particular activity.

This study examined only active motion. Passive joint range of motion would be important to assess because active (voluntary) motion is often limited by joint pain, internal derangement, or by pain associated with inflammation of the ligaments and tendons of the wrist. Future studies should compare active to passive motion, with the therapist manipulating the joint through the available range.

Future studies should look at translatory movements of the wrist and model the wrist as a six degrees-of-freedom model. The assessment of wrist joint kinetics during specific functional activities should also be a concern in future studies.

APPENDIX

APPENDIX I

Joint Coordinate Program

```
edit/sa filein.ted targetA.fil 1 1
edit/sa filein.ted targetB.fil 2 2
edit/sa filein.ted targetC.fil 3 3
edit/sa filein.ted targetD.fil 4 4
edit/sa filein.ted targetE.fil 5 5
edit/sa filein.ted targetF.fil 6 6

spli targetA.fil com1.trx com1.try com1.trz
spli targetB.fil com2.trx com2.try com2.trz
spli targetC.fil com3.trx com3.try com3.trz
spli targetD.fil com4.trx com4.try com4.trz
spli targetE.fil com5.trx com5.try com5.trz
spli targetF.fil com6.trx com6.try com6.trz

subt com6.trx com3.trx vec36.trx
subt com6.try com3.try vec36.try
subt com6.trz com3.trz vec36.trz
subt com5.trx com3.trx vec35.trx
subt com5.try com3.try vec35.try
subt com5.trz com3.trz vec35.trz
subt com2.trx com4.trx vec42.trx
subt com2.try com4.try vec42.try
subt com2.trz com4.trz vec42.trz
subt com1.trx com4.trx vec41.trx
subt com1.try com4.try vec41.try
subt com1.trz com4.trz vec41.trz

mult vec36.try vec35.trz tmp.mul1
mult vec36.trz vec35.try tmp.mul2
subt tmp.mul1 tmp.mul2 vecx.tx
mult vec36.trz vec35.trx tmp.mul1
mult vec36.trx vec35.trz tmp.mul2
subt tmp.mul1 tmp.mul2 vecx.ty
mult vec36.trx vec35.try tmp.mul1
mult vec36.try vec35.trx tmp.mul2
subt tmp.mul1 tmp.mul2 vecx.tz

mult vecx.ty vec36.trz tmp.mul1
mult vecx.tz vec36.try tmp.mul2
subt tmp.mul1 tmp.mul2 vecz.tx
mult vecx.tz vec36.trx tmp.mul1
mult vecx.tx vec36.trz tmp.mul2
subt tmp.mul1 tmp.mul2 vecz.ty
mult vecx.tx vec36.try tmp.mul1
mult vecx.ty vec36.trx tmp.mul2
subt tmp.mul1 tmp.mul2 vecz.tz
```

Joint Coordinate Program(Cont.)

```
mult vec42.try vec41.trz tmp.mul1
mult vec42.trz vec41.try tmp.mul2
subt tmp.mul1 tmp.mul2 vecX.tx
mult vec42.trz vec41.trx tmp.mul1
mult vec42.trx vec41.trz tmp.mul2
subt tmp.mul1 tmp.mul2 vecX.ty
mult vec42.trx vec41.try tmp.mul1
mult vec42.try vec41.trx tmp.mul2
subt tmp.mul1 tmp.mul2 vecX.tz

mult vec42.try vecX.tz tmp.mul1
mult vec42.trz vecX.ty tmp.mul2
subt tmp.mul1 tmp.mul2 vecY.tx
mult vec42.trz vecX.tx tmp.mul1
mult vec42.trx vecX.tz tmp.mul2
subt tmp.mul1 tmp.mul2 vecY.ty
mult vec42.trx vecX.ty tmp.mul1
mult vec42.try vecX.tx tmp.mul2
subt tmp.mul1 tmp.mul2 vecY.tz

squa vecx.tx sqx.tx
squa vecx.ty sqx.ty
squa vecx.tz sqx.tz
add sqx.tx sqx.ty sumx.txy
add sumx.txy sqx.tz sumx.xyz
sqrt sumx.xyz sqrtx.xyz
divi vecx.tx sqrtx.xyz uvix.tx
divi vecx.ty sqrtx.xyz uvix.ty
divi vecx.tz sqrtx.xyz uvix.tz

squa vec36.trx sq36.tx
squa vec36.try sq36.ty
squa vec36.trz sq36.tz
add sq36.tx sq36.ty sum36.txy
add sum36.txy sq36.tz sum36.xyz
sqrt sum36.xyz sqrt36.xyz
divi vec36.trx sqrt36.xyz uviy.tx
divi vec36.try sqrt36.xyz uviy.ty
divi vec36.trz sqrt36.xyz uviy.tz

squa vecz.tx sqz.tx
squa vecz.ty sqz.ty
squa vecz.tz sqz.tz
add sqz.tx sqz.ty sumz.txy
add sumz.txy sqz.tz sumz.xyz
sqrt sumz.xyz sqrtz.xyz
divi vecz.tx sqrtz.xyz uviz.tx
divi vecz.ty sqrtz.xyz uviz.ty
divi vecz.tz sqrtz.xyz uviz.tz

squa vec42.trx sq42.tx
squa vec42.try sq42.ty
squa vec42.trz sq42.tz
add sq42.tx sq42.ty sum42.txy
add sum42.txy sq42.tz sum42.xyz
sqrt sum42.xyz sqrt42.xyz
divi vec42.trx sqrt42.xyz uvIZ.tx
divi vec42.try sqrt42.xyz uvIZ.ty
divi vec42.trz sqrt42.xyz uvIZ.tz
```

Joint Coordinate Program(Cont.)

```
squa vecX.tx sqX.tx
squa vecX.ty sqX.ty
squa vecX.tz sqX.tz
add sqX.tx sqX.ty sumX.txy
add sumX.txy sqX.tz sumX.xyz
sqrt sumX.xyz sqrtX.xyz
divi vecX.tx sqrtX.xyz uvIX.tx
divi vecX.ty sqrtX.xyz uvIX.ty
divi vecX.tz sqrtX.xyz uvIX.tz

squa vecY.tx sqY.tx
squa vecY.ty sqY.ty
squa vecY.tz sqY.tz
add sqY.tx sqY.ty sumY.txy
add sumY.txy sqY.tz sumY.xyz
sqrt sumY.xyz sqrtY.xyz
divi vecY.tx sqrtY.xyz uvIY.tx
divi vecY.ty sqrtY.xyz uvIY.ty
divi vecY.tz sqrtY.xyz uvIY.tz

mult uvIZ.ty uvix.tz tmp.mul1
mult uvIZ.tz uvix.ty tmp.mul2
subt tmp.mul1 tmp.mul2 uve2.tx
mult uvIZ.tz uvix.tx tmp.mul1
mult uvIZ.tx uvix.tz tmp.mul2
subt tmp.mul1 tmp.mul2 uve2.ty
mult uvIZ.tx uvix.ty tmp.mul1
mult uvIZ.ty uvix.tx tmp.mul2
subt tmp.mul1 tmp.mul2 uve2.tz

squa uve2.tx sqe2.tx
squa uve2.ty sqe2.ty
squa uve2.tz sqe2.tz
add sqe2.tx sqe2.ty sume2.txy
add sume2.txy sqe2.tz sume2.xyz
sqrt sume2.xyz sqrte2.xyz
divi uve2.tx sqrte2.xyz uve2.tx
divi uve2.ty sqrte2.xyz uve2.ty
divi uve2.tz sqrte2.xyz uve2.tz

mult uviz.tx uve2.tx devi.tx
mult uviz.ty uve2.ty devi.ty
mult uviz.tz uve2.tz devi.tz
add devi.tx devi.ty devi.txy
add devi.txy devi.tz devi.xyz
asin devi.xyz deviation.asn

mult uvIX.tx uve2.tx flex.tx
mult uvIX.ty uve2.ty flex.ty
mult uvIX.tz uve2.tz flex.tz
add flex.tx flex.ty flex.txy
add flex.txy flex.tz flex.xyz
asin flex.xyz flexion.asn

mult uvix.tx uvIZ.tx rot.tx
mult uvix.ty uvIZ.ty rot.ty
mult uvix.tz uvIZ.tz rot.tz
add rot.tx rot.ty rot.txy
add rot.txy rot.tz rot.xyz
asin rot.xyz rotation.asn
```

BIBLIOGRAPHY

BIBLIOGRAPHY

1. Andrews, J.G., Youm, Y.: A biomechanical investigation of wrist kinematics, J. Biomechanics 12:83-93, 1979.

2. Brumbaugh, R.B., Crowninshield, R.D., Blair, W.F., and Andrews, J.G.: An in-vivo study of normal wrist kinematics, ASME- J. Biomechanical Eng. 104:176-181,1982.

3. Bryce, T.H.: Certain points in the anatomy and mechanism of the human joint reviewed in the light of a series of roentgen ray photographs of the living hand, J. Anat. Physiol. 31:59-67, 1896

4. Carr, L.M.: A method for recording and analyzing labial and gnathic motion in three-dimensions, Master's Thesis, Michigan State University, E. Lansing, MI, 1989.

5. Chao, E.Y.: Justification of triaxial goniometer for the measurement of joint motion, J. Biomechanics, 13:989-1006, 1980.

6. Chao, E.Y.and Morrey, B.F.: Three-dimensional rotation of the elbow, J. Biomechanics 11:57-73, 1978.

7. DeBrunner, H.U.: Orthopaedic Diagnosis, Year Book Medical Publishers, Inc., Chicago, IL, 1982.

8. DeLange, A., VanLeeuwen, C., Kauer, J., Huiskes, R., and Huson, A.: A 3-D kinematic evaluation of a human wrist specimen, Biomaterials and Biomechanics 1983, Elsevier Science Publishers B.V., Amsterdam, 1984.

9. Fick, R.: Handbuch der anatomie und mechanik der gelenke, Teil II, Verlag Gustav-Fischer, Jena, 1910.

10. Gilford, W.W., Bolton, R.H., and Lambrinudi, C.: The mechanism of the wrist joint with special reference to fractures of the scaphoid, Guy's Hosp. Rep. 92:52, 1943.

11. Goldstein, H.: Classical Mechanics, NY: Addison-Westley, pp. 107-109, 1960.

12. Grood, E.S.and Suntay, W.J.: A joint coordinate system for the clinical description of three-dimensional motions: Application to the knee, J. Biomechanical Eng. 105:136-144, 1983.

13. Heck, C.V., Hendryson, I.E., Rowe, C.R.: Joint motion: method of measuring and recording, Amer. Acad. Ortho. Surg., 1965.

14. Hoppenfeld, S.: Physical Examination of the Spine and Extremities, Appleton-Century-Crofts, Norfolk, CT, 1976

15. Kapandji, I.A.: The Physiology of the Joint - The upper Extremity, Churchill Livingstone, New York, NY, 1985.

16. 3M Industrial Optics Products Bulletin, 3M Scotchlite Brand High Gain 7610 and High Contrast 7615 Sheeting Specifications, 1989.

17. MacConnaill, M.A.: The mechanical anatomy of the carpus and its bearing on some surgical problems. J. Anat. 75:166-175, 1941.

18. Mann, K.A., Werner, F.W., and Palmer, A.K.: Frequency spectrum analysis of wrist motion for activities of daily living, J. Ortho. Res. 7:304-306, 1989.

19. Miller, N.R., Shapiro, R. and McLaughlin, T.M.: A technique for obtaining kinematic parameters of segments of biomechanical systems from cinematographic data. J. Biomechanics 100:56-67, 1977.

20. Motion Analysis Corporation, Expertvision* Reference Manual pgs. 23-154. * Expertvision is a registered trademark of Motion Analysis Corp., all right reserved, 1987.

21. Polley, H.F. and Hunter, G.G.: Physical Examination of the Joints. 2nd ed., W.B. Saunders Comp., Philadelphia, PA, 1978.

22. Sommer, H.J. and Miller, N.R.: A technique for kinematic modeling of anatomical joints. ASME - J. Biomechanical Eng. 102:311-317, 1980.

23. Soutas-Little, R.W., Beavis, G.C., Verstraete, M.C., and Markus, T.L.: Analysis of foot motion during running using a joint coordinate system, Medicine and Science in Sports and Exercise, 19:285-293, 1987.

24. Taleisnik, J.: The Wrist, Churchill Livingstone, New York, NY, 1985.

25. Tolbert, J.R., Blair, W.F., Andrews, J.G. and Crowninshield R.D.: The kinetics of normal and prosthetic wrists. J. Biomechanics 18:887-897, 1985.

26. Volz, R.G., Lieb, M. and Benjamin, J.: Biomechanics of the wrist, Clin. Ortho. Rel. Res. 149:112-117, 1980.

27. Walton, J.S.: Close-range cine-photogrammetry: A generalized technique for quantifying Gross human motion. PhD. Dissertation, Pennsylvania State University, May 1981.

28. Walton, J.S.: Personnal correspondence, May 1989.

29. Wright, R.D.: A detailed study of movement of the wrist joint. J. Anat. 70:137-142, 1935.

30. Youm, Y. and Flatt, A.E.: Kinematics of the wrist, Clin.Ortho. Rel. Res. 149:21-32, 1980.

31. Youm, Y., McMurty, R.Y., Flatt, A.E., and Gillespie, T.E.: Kinematics of the wrist, J.B.J.S. 60A:423-431, 1978.

32. Youm, Y. and Yoon, Y.S.: Analytical development in investigation of wrist kinematics. J. Biomechanics 12:613-621, 1979.

General References

1. Chao, E.Y., An, K.N.: Determination of the internal forces in the human hand. J. of Eng. Mech. Div., Proceedings of ASCE 104-NoEM1:255-272, 1979.

2. Erdman, A.G., Mayfield, J.K., Dorman, F., Wallrich,M., and Dahlof, W.: Kinematic and kinetic analysis for the human wrist by stereoscopic instrumentation. ASME- J. Biomechanical Eng. 101:124-131, 1979.

3. Kauer, J.M.: Functional anatomy of the wrist, Clin. Ortho. and Rel. Res. 149:9-20, 1980.

4. Moore, K.L.: Clinically Oriented Anatomy, Williams and Wilkens Company, Baltimore, MD, 1980.

5. Palmer, A.K., Werner, F.W., Murphy, D. and Glisson, R.: Functional wrist motion: a biomechanical study. J. Hand. Surg. (Am) 10:39-49, 1985.